We are IntechOpen,
the world's leading publisher of
Open Access books
Built by scientists, for scientists

4,900
Open access books available

124,000
International authors and editors

140M
Downloads

154
Countries delivered to

Our authors are among the

TOP 1%
most cited scientists

12.2%
Contributors from top 500 universities

CLARIVATE ANALYTICS
BOOK CITATION INDEX
INDEXED

WEB OF SCIENCE™

Selection of our books indexed in the Book Citation Index
in Web of Science™ Core Collection (BKCI)

Interested in publishing with us?
Contact book.department@intechopen.com

8

Diagnosis of Dementia Using
Nuclear Medicine Imaging Modalities

Merissa N. Zeman, Garrett M. Carpenter and Peter J. H. Scott
Department of Radiology, University of Michigan Medical School, Ann Arbor, MI,
USA

1. Introduction

Dementia describes the loss of brain function that occurs with certain diseases, and which has the potential to affect memory, thinking, language, judgment, and behavior. Most types of dementia involve irreversible neurodegeneration, and Alzheimer's disease (AD) is the most common form. Beyond AD however, there are many other diseases that can lead to dementia including dementia with Lewy bodies (DLB), frontotemporal dementia (FTD), Parkinson's disease with dementia, corticobasal degeneration (CBD) and progressive supranuclear palsy (PSP). Dementia can also be the result of many small strokes and, in such cases, is called vascular dementia.

Whilst such clinically and neuropathologically overlapping dementia diseases can be predicted by clinical diagnosis, definitively differentiating them from one another has typically been attempted using high-risk diagnostic procedures (e.g. brain biopsy, Lumbar puncture) or, more commonly, during a *post-mortem* examination. This makes it difficult to a) differentiate dementias and treat each appropriately before patient death; b) manage the diseases early, before the onset of cognitive decline; c) select appropriate patients for assisting in dementia-related drug development; and d) track the impact of new dementia therapeutics in clinical trials. Therefore, new non-invasive diagnostic methods for managing dementia are in high demand and, reflecting this, many radiopharmaceuticals (drugs tagged with a radioactive isotope) have been developed over the last 2 decades that allow non-invasive examination of dementia pathophysiology in living human subjects using nuclear medicine imaging techniques. Such techniques include positron emission tomography (PET) and single photon emission computed tomography (SPECT) imaging, and have greatly enhanced diagnostic confidence across the entire dementia disease spectrum in recent years. This chapter reviews radiopharmaceuticals commonly employed clinically in the management of dementia patients, suffering from the diseases outlined above, with nuclear medicine modalities. The chapter is divided by disease entity, and progress in imaging the pathophysiology of each disease is highlighted. In addition to those radiopharmaceuticals with approval for human use discussed herein, there are many experimental radiopharmaceuticals for dementia in pre-clinical development, which have not yet been translated into clinical use. Comprehensive review of such pre-clinical radiopharmaceuticals is outside the scope of this book, and pertinent examples are highlighted only when necessary to indicate key concepts involved in imaging dementia patients. The interested reader can obtain additional information on radiopharmaceuticals currently in development

for dementia from many excellent and comprehensive review articles available in the literature (Brücke, et al., 2000; Herholz, 2003, 2011; Herholz, et al., 2007; Ishii, 2002; Jagust, 2004; Kadir and Nordberg, 2010; Nordberg, 2004, 2008; Pavese and Brooks, 2009; Sioka, et al., 2010; Vitali, et al., 2008).

2. Alzheimer's disease

2.1 Introduction

Alzheimer's disease (AD) is the most common form of dementia, affecting, for example, 5.3 million Americans, and this number is expected to rise as the baby boom generation comes of age. The cause of AD is presently not entirely understood but what is clear is that it results from a complex neurodegenerative cascade that includes misfolding and aggregation of proteins such as amyloid and tau, with concomitant decline of neurotransmitter systems. As set forth by the National Institute of Neurological and Communicative Diseases and Stroke-Alzheimer's Disease and Related Disorders Association (NINCDS-ADRDA) and the Diagnostic and Statistical Manual of Mental Disorders, fourth edition (DSM-IV-TR), a diagnosis of Alzheimer's disease (AD) requires two components: (1) clinical progressive dementia with episodic memory impairment and (2) hallmark neuropathological changes, including the presence of extracellular Aβ plaques and intraneuronal neurofibrillary tangles (NFTs) in the cortical brain (APA, 2000; McKhann, et al., 1984). Due to the difficulty of confirming histopathology *in vivo*, however, AD can only be definitively diagnosed *post-mortem*. Consequently, the prevailing criteria only allow a probabilistic diagnosis of AD based on clinical phenotype. Specifically, a patient must present with manifest dementia above a certain severity threshold, impairment of two or more cognitive domains, which must cause major interference with social function, and a daily regiment to receive a clinical diagnosis of AD (APA, 2000). After confirming the presence of dementia, a clinician must exclude other conditions that might account for cognitive decline (McKhann, et al., 1984). Since the criteria's enumeration in 1984, new data has emerged - specifically, with regards to the biological basis of AD. New clinical tests, (chiefly, MRI, CT and PET), coupled with the Mini-Mental State Examination (MMSE) and ECG, may foment a clinician's ability to differentiate between forms of dementia.

While clinical-neuropsychological testing remains one of the best tools in a clinician's armamentarium, the utility of such testing is limited in many respects. Evidence suggests that AD pathology (i.e. Aβ deposition in extracellular plaques and vascular walls, tau neurofibrillary tangles (NFTs), cerebral atrophy, synaptic reduction, and neuronal loss) may develop years to decades before the appearance of cognitive deterioration (Pike, et al., 2007; Price and Morris, 1999; Thal, et al., 2002). As dementia represents a late stage in the progression of this disease, early clinical diagnosis of AD is not possible with a great degree of accuracy. Clinical-neuropsychological testing has low sensitivity and specificity in early pre-dementia stages because, in part, a mere subset of individuals that is clinically diagnosed with mild cognitive impairment (MCI), an at-risk population, will progress to AD (Forsberg, et al., 2008; Petersen, et al., 2009; Pike, et al., 2007). Even within later stages, a clinical diagnosis of AD is only probable, not definitive. Only 70 to 90% of persons that match the aforementioned criteria have their diagnoses confirmed at autopsy (Jellinger, et al., 1990; Kukull, et al., 1990). A clinical differential diagnosis of dementia remains somewhat difficult, as many of the cognitive symptoms of AD overlap with those of other neurodegenerative disorders.

It is thus apparent that there is a great need to revise the way in which AD is conceptualized. Accurate and definitive diagnoses need to occur *ante-mortem*, in lieu of *post-mortem*, and preferably in the early pre-dementia (prodromal) stage. Dubois *et al.*, having moved beyond the NINCDS-ADRDA criteria for probable AD, introduced new standards for diagnosis (Dubois, et al., 2007). They include early and significant episodic memory impairment and at least one abnormal *in vivo* biomarker- particularly, medial temporal lobe atrophy, abnormal CSF biomarkers (increased total tau concentrations, increased phospho-tau concentrations, low $A\beta_{1-42}$ concentrations, or a combination of all three), brain $A\beta$ load, temporoparietal hypometabolism on [^{18}F]FDG-PET, and/or specific binding pattern with particular PET ligands. Learning more about AD biomarkers, and how they fit into the accepted paradigm for this disease, will allow for decreased dependence on unreliable clinical diagnostic criteria. Non-invasive PET imaging can be particularly useful in this context. Probes are being developed that target specific AD biomarkers, allowing us to monitor AD pathophysiology *in vivo*. The main strategies for exploration of AD pathophysiology using PET imaging have been reviewed (Jagust, 2004; Nordberg, 2004, 2008), and are outlined in the following sections.

2.2 Imaging Alzheimer's disease with [^{18}F]FDG

[^{18}F]Fluoro-2-deoxy-D-glucose ([^{18}F]FDG) is the most commonly used radiopharmaceutical for clinical PET imaging to date. Patients receive an injection of [^{18}F]FDG, and then images are typically obtained 30 – 60 min later. As a radiolabeled analog of glucose, [^{18}F]FDG is typically employed as a marker of cell proliferation as it preferentially accumulates in cells with increased glucose consumption (e.g. tumors). Therefore, [^{18}F]FDG finds widespread application in oncology including diagnosis and staging of cancers, and monitoring tumor response to chemotherapy. However, glucose is also the main energy supply for the brain and, reflecting this, levels are closely coupled to neuronal function so that measurement of cerebral glucose metabolism can provide diagnostically relevant information about the neurodegenerative disorders described above. According to Herholz and colleagues (Herholz, et al., 2007), typical resting state cerebral metabolic rate for glucose is 40-60 µmol glucose/100 g/min for grey matter, and 15 µmol glucose/100 g/min for white matter, although this does drop off somewhat with age (Kuhl, et al., 1982). Observed regional differences include higher values in the striatum and parietal cortex. Other phylogenetically older brain structures (e.g. medial temporal cortex and cerebellum) have glucose metabolism rates between grey matter and white matter.

For at least two decades, significant efforts have been made to image patients at various stages of Alzheimer's disease (including high risk, asymptomatic patients; patients with mild cognitive impairment (MCI); and patients with fully developed Alzheimer's disease) with [^{18}F]FDG (e.g. Figure 1). In patients considered high risk for developing AD (for example because of family history and possession of the ApoE ε4 allele (Reiman, et al., 1996; Small, et al., 1995)), impairment of regional cerebral glucose metabolism has been observed decades before likely onset of dementia and certainly while the patients are still asymptomatic (Reiman, et al., 2004).

In 1997, Kuhl and colleagues reported the first example of using posterior cingulate glucose metabolism, determined from [^{18}F]FDG PET scans, to predict progression of disease in patients with MCI (Minoshima, et al., 1997). The results have been echoed by a number of subsequent longitudinal studies, which have confirmed the high predictive power of
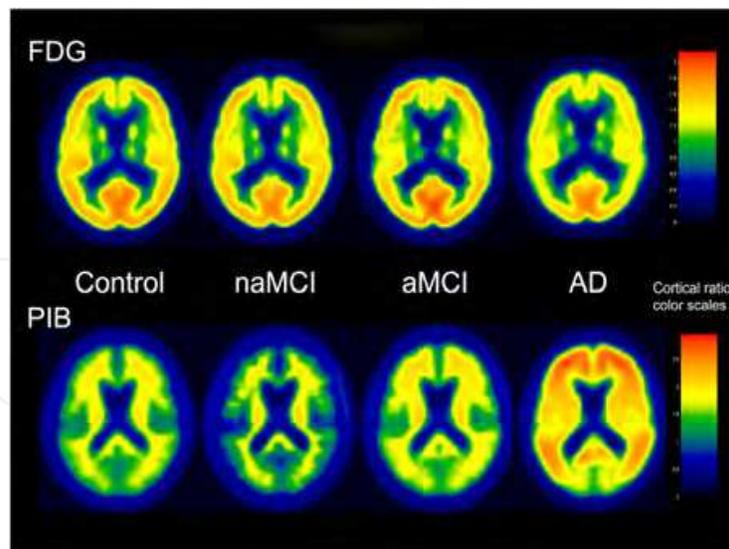
Fig. 1. 18F-FDG and PiB group mean images for control, naMCI, aMCI, and AD subjects showing better visual separation of groups using PiB. Scaling shown to right using pons and cerebellar normalization, respectively. Regions with activity similar to these regions of normalization color in 1.0 color ranges (green), whereas regions with greater uptake show up in yellow and red. Color scaling is slightly different for 18F-FDG and PiB groups given different range of cortical ratios. *(Reprinted with permission from Loew VJ, Kemp BJ, Jack CR, et al. Comparison of 18F-FDG and PiB PET in Cognitive Impairment. J Nucl Med. 2009;50:878-886)*

[18F]FDG PET. For example, Berent and colleagues reported 70% progression of disease in 3 years following an abnormal PET scan, but only 30% progression after a normal PET scan (Berent, et al., 1999). Anchisi and co-workers also showed that a normal FDG PET scan indicated low chance of progression of MCI into full AD within 1 year (Anchisi, et al., 2005). Generally speaking [18F]FDG PET has >80% sensitivity and specificity for prediction of rapid progression. Moreover, a recent report by Drzezga and colleagues discovered that [18F]FDG PET (92% sensitivity, 89% specificity) was superior to ApoE ε4 testing (75% sensitivity, 56% specificity) when used to predict disease progression (A. Drzezga, et al., 2005). Other aspects of [18F]FDG PET scans have also proven pertinent to the assessment of MCI. For example, mesial temporal metabolic impairment (Heiss, et al., 1992), as well as hippocampal and antorhinal metabolic impairment (de Leon, et al., 2001), although the latter can be difficult to assess because of small size.

As MCI progresses and develops into Alzheimer's disease, numerous studies over the last two decades have shown that both cerebral blood flow and glucose metabolism are reduced in a number of areas of the brain. For example, impairment of glucose metabolism in the temporoparietal association cortices is typical in AD (on the order of 16-19% over 3 years (Smith, et al., 1992)), whilst no significant decline is apparent in the corresponding normal controls. These cortices are also prone to amyloid deposition during AD (Bartzokis, et al., 2007). Reduced glucose metabolism may also occur in the frontal association cortex, although more so as AD progresses. In contrast to the other dementia diseases discussed herein, the rate of glucose metabolism in other areas of the brain including the visual and motor cortex, basal ganglia and cerebellum is unaffected (Herholz, et al., 2007). This is in agreement with the clinical manifestation of AD, as primary motor and sensory function remain intact, whilst memory, associative thinking, planning of action and other higher

sensory processing decline. Such clinical and imaging differences can be used as a means of differentiating AD from other related disorders.

More subtle differences between FDG PET scans of normal patients and AD patients are also apparent if more advanced image analysis is employed. Voxel-based analysis can detect differences in FDG PET that are not obvious upon visual interpretation of the scan. For example, comparison of FDG PET scans of AD patients versus normal controls reveals impaired glucose metabolism in the posterior cingulate gyrus as well as the precuneus (Minoshima, et al., 1997). This is not immediately obvious because metabolism in these areas is normally above average and the decrease in AD patients can obscure it into the background. The large amounts of FDG PET data obtained in AD patients now allow advanced analytical techniques to go one step further, and automatically detect the typical pattern of metabolic abnormalities associated with AD. This approach has been successfully used to distinguish AD patients for normal controls with >80% (and frequently >90%) accuracy, and such data have enabled the use of FDG PET in AD therapeutic trials (Heiss, et al., 1994).

2.3 Imaging amyloid-ß (Aß) plaque burden in Alzheimer's disease

As $A\beta$ deposition is considered a hallmark neuropathological sign of AD and is thought to be one of the primary events in the pathogenesis of AD (the "amyloid cascade hypothesis"), $A\beta$ PET imaging agents are at the forefront of this expanding field (Haass and Selkoe, 2007). In AD patients, $A\beta$ deposits are composed of $A\beta_{1-40}$ and $A\beta_{1-42}$, peptides that are 40 and 42 amino acids in length, respectively, generated from the sequential proteolytic cleavage of amyloid precursor protein (APP) by β- and γ-secretases (Beyreuther and Masters, 1991; Martins, et al., 1991). Whilst $A\beta_{1-42}$ deposits have a higher propensity to oligomerize, both isoforms are found in fibrillar amyloid plaques (Tamaoka, et al., 1994), characteristic β-sheet-rich structures that represent the target for $A\beta$ PET ligands.

The ability to image and measure $A\beta$ load *in vitro* has considerable implications for the future study of AD. As $A\beta$ deposition commences long before the onset of cognitive deficits, $A\beta$-targeting probes may support earlier diagnoses and interventions in the pre-dementia stage of this disease (Pike, et al., 2007; Price and Morris, 1999; Thal, et al., 2002). $A\beta$ PET imaging additionally has some utility in accurately differentiating AD from $A\beta$-negative forms of dementia and, thus, in increasing the specificity of a clinical diagnosis. Objectively monitoring treatments and selecting candidates for particular drugs and clinical trials are other potential uses for this imaging technology (Rafii and Aisen, 2009); for example, patients with low cortical $A\beta$ load, as measured by $A\beta$ PET, are unlikely to qualify for anti-amyloid therapies.

Due to the large number of possible clinical applications, there has been a dramatic rise in the number of probes that target $A\beta$ plaques over the last decade. The four $A\beta$ PET imaging agents under active commercial development are [11C]PIB, [18F]flutemetamol, [18F]florbetaben, and [18F]florbetapir. Each imaging agent is currently undergoing FDA-approved Phase III clinical trials in the US, except [18F]Florbetapir, which is awaiting FDA approval. Each $A\beta$ PET imaging agent will be discussed individually in further detail below.

2.3.1 [11C]Pittsburgh Compound B ([11C]PiB)

The most well-characterized and studied radiopharmaceutical for $A\beta$ pathology is [11C]Pittsburgh Compound B ([11C]PiB, (N-methyl-[11C])2-(4′-methylamino-phenyl)-6-OH-

BTA), a 6-hydroxyl-substituted benzothiazole aniline; a team led by Mathis and Klunk developed this ^{11}C-labeled neutral derivative of Thioflavin-T amyloid dye at the University of Pittsburgh in 2002 (W. E. Klunk, et al., 2001; Mathis, et al., 2002). Pre-clinical studies of [11C]PiB have demonstrated that this radiotracer has excellent brain penetration (approximately 7% injected dose per gram at 2 minutes post injection) and initial brain uptake, rapid clearance from normal brain tissue, high binding affinity to Aβ plaques (K_i=0.87±0.18 nM), and moderate lipophilicity (W. E. Klunk, et al., 2001; Mathis, et al., 2002; Mathis, et al., 2003). As a carbon-11 labeled ligand, [11C]PiB has the advantage of delivering a lower radiation burden (whole-body effective dose conversion factor for a 70-kg adult= 4.74±0.8 μSv/MBq; typical administered dose= 489±61 MBq (13±1.65 mCi); effective dose= 2.37±0.53 mSv). Furthermore, [11C]PiB is able to reach a maximum effect size more rapidly than ^{18}F-labeled radiopharmaceuticals, leading to shorter imaging times (50-70 minutes as the optimal time-window) (McNamee, et al., 2009; O'Keefe, et al., 2009; Scheinin, et al., 2007). Of particular interest, *in vitro* autoradiography studies have confirmed that [11C]PiB binds to aggregated, fibrillar Aβ deposits in the cortex, striatum, and cerebral vessel walls, but not to amorphous, cerebellar Aβ deposits (Greenberg, et al., 2008; W. E. Klunk, et al., 2003; Lockhart, et al., 2007). At nanomolar concentrations, however, [11C]PiB does not bind to free soluble amyloid, NFTs, or Lewy bodies (Fodero-Tavoletti, et al., 2007; W. E. Klunk, et al., 2003; Lockhart, et al., 2007).

In 2004, Klunk *et al.* published the results from their first in human proof-of-mechanism study (W. E. Klunk, et al., 2004). With 16 mild AD patients and 9 healthy controls, this study supported the use of [11C]PiB uptake patterns for the reliable discrimination between the two diagnostic groups. AD patients had a twofold increase of [11C]PiB uptake over healthy controls, as measured by regional and average neocortical standard uptake value ratios (SUVRs) with the cerebellum as the reference region, specifically in the frontal, temporal, parietal, and lateral temporal cortices, portions of the occipital cortex, and the striatum. This pattern of [11C]PiB uptake is consistent with the distribution of Aβ plaques in previous *post-mortem* studies (Thal, et al., 2002). Three AD patients, however, had [11C]PiB retention levels in the range typical for healthy controls. Contrastingly, all healthy controls, except one, showed little or no cortical [11C]PiB binding. Non-specific binding was present in white matter areas, but at identical levels in healthy controls and AD patients. This study additionally cited a significant inverse correlation between [11C]PiB uptake and cerebral metabolic rate, especially in the parietal cortex, but only when healthy controls and AD patients were pooled together. Despite this significant trend, [11C]PiB uptake levels provided higher discriminatory power than cerebral metabolic rate in differentiating AD patients from healthy controls.

Since this groundbreaking study, the number of investigations using [11C]PiB in humans, as well as research applications for this radiopharmaceutical, have greatly proliferated. Numerous studies have been dedicated to determining the relationship between [11C]PiB retention and other AD biomarkers, as well as clinical features/parameters. For example, [11C]PiB uptake negatively correlates with CSF $Aβ_{1-42}$ levels in AD patients and healthy controls (Fagan, et al., 2007; Forsberg, et al., 2010). Furthermore, tracer binding is directly proportional to CSF tau in MCI patients, but not AD patients, cerebral atrophy as measured by MRI in AD subjects (although NFTs correlate better), and temporoparietal hypometabolism as measured by [18F]FDG-PET (Forsberg, et al., 2008; W. E. Klunk, et al., 2004; Storandt, et al., 2009). In addition, subjects with at least one Apolipoprotein E ε4 (ApoE

ε4) allele, a genotype strongly associated with AD, are more likely to have a [11C]PiB-positive scan than a negative one (A. Drzezga, et al., 2009; Storandt, et al., 2009).

While [11C]PiB has primarily shown utility in differentiating AD patients from healthy controls, this tracer has also been assessed for the differential diagnosis of dementia. [11C]PiB binding patterns allow for great separation between AD and Frontotemporal Lobar Degeneration (FTLD) patients, as those with the frontotemporal and semantic forms of the latter rarely have Aβ plaques *post-mortem* (A. Drzezga, et al., 2008; Engler, et al., 2008; Rabinovici, et al., 2007; Rowe, et al., 2007). Contrastingly, due to the presence of Aβ deposits in a large proportion of patients with Lewy body dementia (DLB) (only 15% of cases represent "pure" DLB with no Aβ pathology), it is harder to distinguish DLB from AD solely based on [11C]PiB binding alone (McKeith, et al., 1996; Rowe, et al., 2007). In comparison to the distribution pattern typical of AD patients, DLB cortical [11C]PiB uptake has been noted to be more variable and lower in a majority of cases (Rowe, et al., 2007). While [11C]PiB cannot distinguish AD and DLB pathology with a high degree of accuracy, this technology could potentially be used to identify Aβ-negative and Aβ-positive DLB subsets. Whether this discrimination signifies differences in therapeutic options remains unknown at this time. In a study by *Rowe et al.*, the presence of Aβ deposition (high Aβ load) was associated with a more rapid onset of the full DLB phenotype (Rowe, et al., 2007). [11C]PiB studies, thus, may be able to shed new insights into DLB pathophysiology. Healthy controls have been additional subjects of [11C]PiB studies because 10-30% of cognitively normal elderly people have Aβ plaques at levels comparable to those of AD patients *post-mortem* (Aizenstein, et al., 2008; Price and Morris, 1999). Concomitantly, 10-30% of healthy controls with normal cognition show increased cortical [11C]PiB binding (W. E. Klunk, et al., 2004; Mintun, et al., 2006; Morris, et al., 2009; Rowe, et al., 2007). To date, this technology does not allow discrimination between healthy controls with high Aβ load and AD patients. The meaning of these false-positive scans is unclear; while low specificity is possible, high [11C]PiB uptake and thus Aβ load in cognitively normal people most likely represents either pre-clinical AD or "benign" pathology (Mintun, et al., 2006; Morris, et al., 2009; Rowe, et al., 2007).

There is evidence to suggest a prodromal stage of AD does exist, in which Aβ deposition begins in a small subset of adults as a primary event (Jack, et al., 2009; Pike, et al., 2007; Rowe, et al., 2007). As these individuals reach the MCI phase, the amount of Aβ accumulation approximates the levels seen in AD patients (Jack, et al., 2009; Pike, et al., 2007). Upon conversion to AD, Aβ load either plateaus or progresses slowly. Consequently, clinical cognitive decline (or severity of dementia) does not correlate with Aβ load, as measured *in vivo* by [11C]PiB (Jack, et al., 2009; Rowe, et al., 2007). This time course for Aβ accumulation is further supported by a 2-year study in which a majority of 16 AD subjects did not show a significant change in [11C]PiB uptake from baseline, despite decreases in clinical cognitive parameters and temporoparietal metabolism (as measured by [18F]FDG-PET) (Engler, et al., 2006). The results from this study support the use of [11C]PiB as a potential early biomarker for AD, but not as an indicator of disease severity. Other measures, such as [18F]FDG-PET and tau PET imaging agents, which track later-developing biomarkers, correlate better with cognitive decline and thus can be used to assess neurodegeneration (Meyer, et al., 2011).

To further evidence [11C]PiB's ability to act as an early biomarker for AD, radiotracer studies have been performed in MCI patients. [11C]PiB distribution patterns in MCI patients are

dichotomous, with one subset of MCI patients showing abundant "AD-like" neocortical binding ([11C]PiB-positive) and the other subset showing low, non-specific binding ([11C]PiB-negative) (Forsberg, et al., 2008; Okello, et al., 2009; Pike, et al., 2007; Rowe, et al., 2007). As only 40-60% of MCI patients progress to AD, longitudinal studies are needed to determine if this bimodal distribution pattern of [11C]PiB uptake accurately predicts those who will convert to AD (Forsberg, et al., 2008; Kukull, et al., 1990; Okello, et al., 2009; Petersen, et al., 2009). In a study by Forsberg *et al.*, 7 out of 21 tested MCI patients converted to AD after 8.1±6.0 months (Forsberg, et al., 2008). Interestingly, there were detectable group differences between the 7 MCI converters and the 14 non-converters. MCI converters were shown to have lower levels of CSF $A\beta_{1-42}$ and MMSE test scores compared to non-converters. Additionally, MCI converters were more likely to be ApoE ε4 carriers (85%) than were non-converters (57%). Most importantly, MCI converters had high [11C]PiB uptake in the frontal, parietal, and temporal cortices and the posterior cingulum, similar to levels in AD patients. Contrastingly, MCI non-converters had significantly lower cortical [11C]PiB retention, indistinguishable from healthy controls. These promising results demonstrate the prognostic value of [11C]PiB for predicting which MCI patients will progress to AD.

[11C]PiB has now been used in a large number of subjects, consistently showing high sensitivity and specificity in detecting cerebral amyloid deposition *in vivo* with high intra- and inter-reader agreement (W. E. Klunk and Mathis, 2008). Due to the short physical half-life of carbon-11 (20.4 minutes), however, [11C]PiB is limited in clinical availability. As a result, Aβ tracers that are radiolabeled with fluorine-18, a radioisotope with a considerably longer half-life (109.4 minutes) than carbon-11, have been developed. Fluorine-18 labeled Aβ PET tracers do not require on-site cyclotrons for their production, thus allowing for a more widespread distribution of this imaging technology.

2.3.2 [18F]Flutemetamol (3'-[18F]F-PiB or [18F]GE067)

[18F]Flutemetamol (3'-[18F]F-6-OH-BTA1) is an 18F-labeled thioflavin analog of [11C]PiB licensed to GE Healthcare (Koole, et al., 2009). Due to its longer physical half-life in comparison to its parent molecule, [18F]flutemetamol can potentially have a larger impact in clinical and research settings. Unlike other 18F-labeled Aβ PET radiotracers, [18F]flutemetamol has the advantage that there has been extensive work done on its parent molecule, [11C]PiB, which can easily lend itself to the validation of [18F]flutemetamol. Although [11C]PiB and [18F]flutemetamol exhibit similarities in structure, the two radiotracers have slightly different properties. Fortunately, pre-clinical studies of [18F]flutemetamol have demonstrated favorable brain kinetics, good penetration of intact blood-brain barrier (BBB), and fairly rapid washout of non-specific binding (Nelissen, et al., 2009). [18F]Flutemetamol has showed a good safety profile and biodistribution (Koole, et al., 2009). The average typical administered dose is 121 MBq (range=96-147 MBq; 2.59-3.98 mCi) (Koole, et al., 2009); It is important to note that [18F]flutemetamol delivers an effective dose that is 1.7 times larger than that for [11C]PiB (2.37 mSv versus 4.12 mSv) (O'Keefe, et al., 2009); this higher radiation burden is due to the relatively greater radiation dose associated with fluorine-18 (whole-body effective dose conversion factor= 33.6 μSv/MBq for [18F]flutemetamol versus 4.74±0.8 μSv/MBq for [11C]PiB). Nevertheless, there have been no adverse events reported for the use of this radiotracer and, therefore, it has been deemed safe for use in humans (Koole, et al., 2009).

Under the direction of Nelissen and co-workers, [18F]flutemetamol entered Phase I clinical trials in 2009 (Nelissen, et al., 2009). Eight AD patients and 8 healthy controls were used in

this proof-of-concept study. After 80 minutes post injection, most regions of the neocortex showed a large difference in SUVRs (with the cerebellum as the reference region) between AD patients and healthy controls, except in the medial temporal cortex, which is more prone to NFT buildup than amyloid deposition, and the occipital cortex. This spatial distribution of [18F]flutemetamol uptake in AD patients closely resembles that typically seen in its parent molecule, [11C]PiB. Interestingly however, non-specific binding in white matter was more pronounced, but not statistically significant, in healthy controls injected with [18F]flutemetamol in comparison to when using [11C]PiB (Fodero-Tavoletti, et al., 2009).

While this study showed that [18F]flutemetamol PET imaging can be used to differentiate AD patients and healthy controls, 2 AD patients had particular regional SUVRs within the range seen in healthy controls. These results are comparable to previous [11C]PiB studies, in which 10-20% of clinically diagnosed AD patients did not show high cortical tracer uptake (W. E. Klunk, et al., 2004). Conversely, one healthy control had cortical SUVRs in line with those seen in AD patients. One possible explanation is that high white matter binding led to increased cortical values. The proportion of [18F]flutemetamol-positive healthy controls in this study, however, is comparable to the 10-30% of elderly healthy controls who have increased [11C]PiB brain uptake at levels indistinguishable from AD patients.

Based on the positive Phase I results, [18F]flutemetamol continued to be investigated in a clinical Phase II capacity (Vandenberghe, et al., 2010). Twenty-seven patients with clinically probable AD, 20 patients with amnestic MCI, 15 elderly healthy controls, and 10 younger healthy controls were used to determine the efficacy of blinded visual assessments of [18F]flutemetamol scans as well as to directly measure [18F]flutemetamol against its parent molecule [11C]PiB in terms of its discriminatory power. Researchers found that mean SUVRs in the frontal cortex, lateral temporal cortex, parietal cortex, anterior/posterior cingulate, and striatum were significantly higher in AD patients than in the elderly healthy controls. These results are consistent with the Phase I clinical study for [18F]flutemetamol. Based on blinded visual assessments of [18F]flutemetamol scans, 25 of 27 scans from AD subjects and 1 of 15 scans from the elderly healthy controls were PET-positive, corresponding to a sensitivity of 93.1% and a specificity of 93.3% against the clinical standard of truth. For MCI patients, 9 of 20 subjects were assigned to the high tracer uptake category. The proportion of [18F]flutemetamol-positive scans for MCI patients is comparable to that reported for [11C]PiB (Forsberg, et al., 2008). Additionally, investigators found that the test-retest variability ranged from 1 to 4%, which is lower than that reported for [11C]PiB. Most important to the validation of this radiotracer is that both visually and quantitatively, [18F]flutemetamol uptake was highly concordant with that of [11C]PiB for both AD and MCI patients. However, non-specific binding was greater with [18F]flutemetamol. Regardless, as was seen in Phase I clinical studies, high white matter uptake did not lead to any misclassifications of the scans by the visual readers.

Before clinical application, flutemetamol PET imaging needs to be tested against histopathology findings at autopsy. Thus, GE Healthcare is currently organizing and recruiting for an ongoing [18F]flutemetamol Phase III clinical study (Clinical Trial NCT01165554) that will include patients willing to undergo *post-mortem* studies. Results from this trial are pending (GEHC, Accessed 2011).

2.3.3 [18F]Florbetaben ([18F]BAY94-9172 or [18F]AV-1/ZK)

[18F]Florbetaben ([18F]BAY94-9172, previously [18F]AV-1/ZK, *trans*-4-(N-methyl-amino)-4'-[2-[2-(2-[18F]fluoro-ethoxy)-ethoxy]-ethoxy]-stilbene) is a fluorinated polyethylene glycol

(PEG) stilbene derivative that was developed by Zhang *et al.* in 2005 through Avid Radiopharmaceuticals under the name [18F]AV-1/ZK (Zhang, et al., 2005a). Due to their high binding affinities to Aβ aggregates, stilbene derivatives have been considered as potential Aβ-targeting probes for PET imaging (H. F. Kung, et al., 2001; Zhang, et al., 2005a; Zhang, et al., 2005b). Stilbene derivatives have similar structural characteristics as benzothiazoles (PiB derivatives) and thus compete for the same binding site on amyloid plaques (Zhang, et al., 2005b). [18F]Florbetaben was chosen from a series of stilbenes for its appropriate lipophilicity, high binding affinity (K_i= 6.7±0.3 nM), good safety profile, high initial uptake and rapid washout in normal mouse brain (4 minutes post-injection), and being 18F-radiolabeled (Barthel, et al., 2010; H. F. Kung, et al., 2001; Patt, et al., 2010). The typical administered dose for [18F]florbetaben is 350 MBq (9.5 mCi), and the effective dose is 5.13 mSv using this dose (whole-body effective dose conversion factor= 14.67±1.39 µSv/MBq) (O'Keefe, et al., 2009). However, [18F]florbetaben causes a much lower radiation burden than most other 18F-labeled probes, such as [18F]flutemetmol (Koole, et al., 2009). *In vivo* autoradiography of transgenic mouse brain and *in vitro* autoradiography of *post-mortem* human AD brain tissues have demonstrated specific [18F]florbetaben binding to neuritic Aβ plaques and to cerebral amyloid angiopathy (Zhang, et al., 2005b); [18F]florbetaben does not label Lewy bodies, Pick bodies, glial cytoplasmic inclusions, α-synuclein, NFTs, or other tau pathology to any appreciable extent (Zhang, et al., 2005b). Due to convincing pre-clinical data, [18F]florbetaben entered clinical trials, under the license of Bayer Schering Pharma.

Rowe *et al.* performed the first-in-man proof of mechanism study in 2008, using 15 elderly healthy controls, 15 patients with probable AD, and 5 patients with frontotemporal lobe degeneration (FTLD) (Rowe, et al., 2008). AD patients showed extensive cortical [18F]florbetaben uptake while healthy controls and FTLD patients only demonstrated non-specific binding in white matter, but at levels comparable to those of AD patients. Visual assessment of [18F]florbetaben scans correctly differentiated AD patients from both healthy controls and FTLD patients in all but two cases, leading to a sensitivity and specificity of 100% and 90%, respectively. Results for this study are comparable with previous [11C]PiB studies, in terms of radiotracer distribution. However, the amount of tracer uptake is slightly higher for [11C]PiB. At 90-120 minutes post-injection, the mean neocortical SUVR, with the cerebellum as the reference region, for [18F]florbetaben was 57% greater in AD patients than in healthy controls; but in comparison, [11C]PiB binding is, on average, 70% higher in AD patients than in healthy controls (Rowe, et al., 2007). Nevertheless, [18F]florbetaben PET imaging was shown to be highly sensitive and specific in discriminating between AD patients, healthy controls, and FTLD patients, at a level similar to [11C]PiB.

Subsequent studies have confirmed [18F]florbetaben's high discriminatory power, low inter- and intrareader variability, and clinical utility (Barthel, et al., 2010). As an optimal imaging agent, [18F]florbetaben reaches maximum effect size fairly quickly (90 minutes post-injection) and maintains this contrast for up to 4 hours post-injection (Barthel, et al., 2010; Rowe, et al., 2007). This implies a certain flexibility of the imaging time window, which is advantageous in the clinical arena. [18F]Florbetaben has also been useful in better clarifying the relationship between Aβ load and other AD biomarkers. For example, regional radiotracer uptake, particularly in the lateral temporal cortex, is slightly, but significantly inversely proportional to MMSE and word-list memory scores when AD patients and healthy controls are pooled together (Barthel, et al., 2011; Rowe, et al., 2007). Moreover, there

is a higher frequency of ε4 allele(s) of apolipoprotein E (APOE ε4), a strong risk factor for the development of AD, in AD patients with [18F]florbetaben-positive scans than in those with [18F]florbetaben-negative scans (Barthel, et al., 2011). These results are comparable to findings using [11C]PiB.

Barthel *et al*. reported the largest study to date, using 81 patients with probable AD and 69 healthy controls in the primary analysis (Barthel, et al., 2011). This Phase II study confirmed the diagnostic accuracy and efficacy of [18F]florbetaben in a larger cohort of subjects. Neocortical tracer uptake was significantly higher for AD patients compared with healthy controls in frontal, temporal, parietal and occipital cortices, and anterior / posterior cingulate. On a regional level, the posterior cingulate presented the greatest separation between AD patients and healthy controls and, thus, allowed for the differentiation between the two diagnostic groups. These results are consistent with previous [11C]PiB studies that have shown that tracer uptake in the posterior cingulate is a good and early indicator of probable AD (Ziolko, et al., 2006). Visual assessment of [18F]florbetaben scans have a sensitivity of 80% and specificity of 91% for distinguishing AD patients from healthy controls. Upon statistical adjustment, due to the fact that somewhat unreliable clinical diagnoses (70-90% accuracy) were used as the standard of truth, the sensitivity increased to 96% while the specificity was determined to be 97%.

While Phase II clinical trial showed promising results, [18F]florbetaben imaging needs to be compared to *post-mortem* studies to validate this technique. As of November 30, 2009, [18F]florbetaben has entered Phase III FDA-approved clinical studies in the US (Bayer, Accessed 2011). Using approximately 232 individuals, this trial (Clinical Trial NCT01020838) will assess the efficacy of [18F]florbetaben PET imaging for detection of cerebral Aß against the golden standard of *post-mortem* histopathology. The trial is not expected to be completed until April 2014.

2.3.4 [18F]Florbetapir ([18F]AV-45 or Amyvid)

[18F]Florbetapir ([18F]AV-45, (E)-2-(2-(2-(2-[18F]fluoroethoxy)ethoxy)ethoxy,)-5-(4-methylaminostyryl)pyridine, Amyvid) was recently developed by Avid Radiopharmaceuticals. As a fluoropegylated stilbene derivative, [18F]Florbetapir is similar in structure to [18F]florbetaben, but the stilbene backbone has been replaced with a styrylpyridine core (Zhang, et al., 2007; Zhang, et al., 2005a). [18F]Florbetapir was chosen from a small number of 18F-labeled styrylpyridine analogs due to its optimum *in vivo* kinetics and high selectivity for Aβ plaques (Zhang, et al., 2007). Pre-clinical characterization of [18F]florbetapir demonstrated that this radiotracer has excellent binding affinity (K_d=3.72±0.30 nM) to Aβ aggregates, moderate lipophilicity, high initial brain uptake (7.33±1.54% injected dose per gram at 2 min post-injection) and rapid washout kinetics (1.88±0.14% injected dose per gram remaining in the brain 60 minutes post injection) in normal mice and primate brain (Choi, et al., 2009). Additionally, as supported by *in vitro* autoradiography of *post-mortem* human brain tissue sections and *ex vivo* autoradiography of transgenic mouse brain, [18F]florbetapir selectively labels fibrillar Aβ plaques, but not tau NFTs (Choi, et al., 2009; Choi, et al., 2011). Non-specific binding is low or non-existent. This spatial distribution of [18F]florbetapir uptake is similar to the pattern observed for [18F]florbetaben (Zhang, et al., 2005b).

Favorably, [18F]florbetapir also exhibits fast brain kinetics comparable to that of [11C]PiB (McNamee, et al., 2009). The signal-to-noise ratio for this radiotracer asymptotes at 50-60

minutes post injection and remains stable until at least 90 minutes post-injection (Wong, et al., 2010); contrastingly, both [18F]flutemetamol and [18F]florbetaben reach maximum effect size at 85-90 minutes post injection (Barthel, et al., 2010; Nelissen, et al., 2009). This property of [18F]florbetapir creates a large time-frame to obtain a 10 minute image and allows for shorter imaging times, if necessary. Moreover, [18F]florbetapir has a good safety profile and biodistribution. The typical administered dose is 382.0±14 MBq (10.3±0.38 mCi), and the effective dose is 6.66±0.38 mSv using an administered dose of 370 MBq (whole-body effective dose conversion factor = 18.0±1.01 µSv/MBq) (Lin, et al., 2010). As expected, [18F]florbetapir delivers a higher radiation burden than [11C]PiB, but still within the normal range for 18F-labeled radiopharmaceuticals (O'Keefe, et al., 2009); and thus it remains suitable for clinical imaging applications.

Clinical studies of [18F]florbetapir have consistently shown its high discriminatory power in being able to differentiate between AD patients, patients with amyloid positive and amyloid negative MCI, and healthy controls (e.g. Figure 2) (Lister-James, et al., 2011). For example, in a study of 15 elderly healthy controls and 11 AD patients, [18F]florbetapir uptake was significantly higher in AD patients than in healthy controls, especially in cortical target areas, such as the frontal and temporal cortices and the precuneus (Wong, et al., 2010). Variable tracer uptake was seen in the occipital cortex, in which Aβ deposition is thought to occur inconsistently. Contrastingly, healthy controls had tracer accumulation predominantly in white matter areas, as non-specific binding. It was noted, however, that two elderly healthy controls presented with increased tracer accumulation, indistinguishable from AD patients, and two other healthy controls had borderline levels of tracer uptake, especially in the precuneus. This finding is consistent with previous [11C]PiB studies, in which 10-30% of
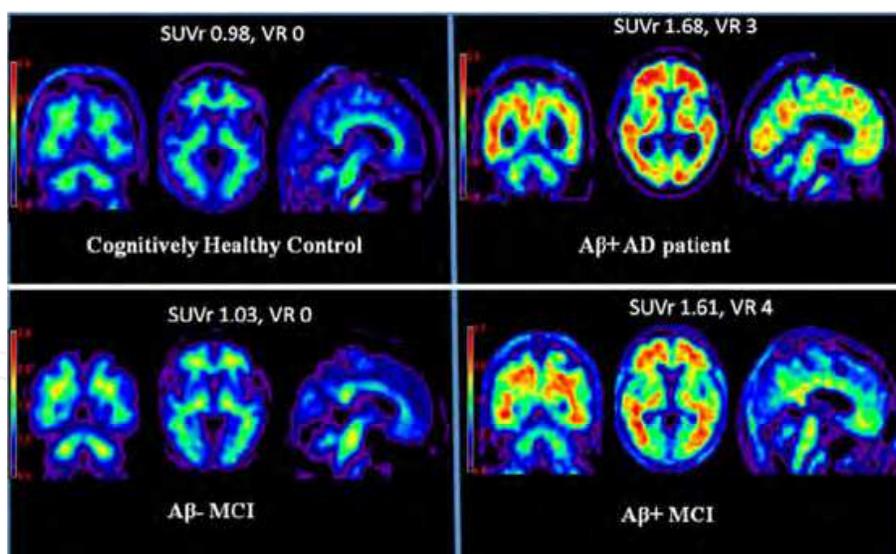

Fig. 2. Florbetapir F-18 PET imaging (coronal, axial, and sagittal views). Top left, healthy control (SUVR = 0.98; visual read score = 0); top right: patient with clinically diagnosed AD and interpreted as Aß+ (SUVR = 1.68; visual read score = 3); bottom left, patient with mild cognitive impairment and interpreted as Aß- (SUVR = 1.03; visual read score = 0); bottom right, patient with mild cognitive impairment and interpreted as Aß+ (SUVR = 1.61; visual read score = 4). *(Reprinted with permission from Lister-James J, Pontecorvo MJ, Clark C, et al. Florbetapir F-18: A histopathologically validated beta-amyloid positron emission tomography imaging agent. Semin. Nucl. Med. 2011;50:300-304)*

cognitively intact healthy subjects have increased tracer uptake (W. E. Klunk, et al., 2004; Mintun, et al., 2006; Morris, et al., 2009; Rowe, et al., 2007).

Lin and co-workers presented similar results for [^{18}F]florbetapir in a clinical study, using 6 healthy controls and 3 AD patients (Lin, et al., 2010). Tracer uptake was particularly high in the frontal, parietal, and occipital cortices of AD patients; healthy controls showed substantial non-specific binding in subcortical white matter. Consequently, simple semi-quantitative measures (SUVRs with the cerebellum as the reference region) could be used to discriminate between AD patients and healthy controls. Of importance, one AD patient showed little uptake of the radiotracer, similar to the binding pattern of healthy controls. This negative scan may be due to a lack of tracer sensitivity, but more likely is indicative of a low Aβ load in this clinically diagnosed AD patient.

In 2011, Clark *et al.* published the results from the first study of its kind, comparing the efficacy of an Aβ PET imaging agent against the golden standard of neuropathology confirmation at autopsy (Clark, et al., 2011b). This study included individuals near end of life who consented to donating their brain after death. Thirty-six subjects with clinically diagnosed AD were included in the autopsy cohort (but only 29 were included in the primary analysis) while 74 young healthy controls were in the non-autopsy cohort. All 74 young healthy controls were found to have a [^{18}F]florbetapir-negative scan. For the primary analysis autopsy cohort, visual assessment scores of [^{18}F]florbetapir scans and average neocortical and regional SUVRs (cerebellum as reference region) correlated well with *post-mortem* amyloid pathology (as measured by immunohistochemistry and silver stain neuritic plaque score).

Interestingly, only 15 participants met pathological criteria for AD in the primary analysis autopsy cohort. Of these 15 participants, 14 had [^{18}F]florbetapir PET scans visually assessed as positive, giving a sensitivity of 93%. Fourteen participants in the primary analysis autopsy cohort had histologically-confirmed low levels of Aβ aggregation at *post-mortem* and thus did not meet the criteria for AD. All 14 participants had [^{18}F]florbetapir-negative scans, leading to a specificity of 100%. This study also cited good interreader agreement among the three nuclear medicine physicians who visually rated the [^{18}F]florbetapir PET images ($0.68 \leq \kappa \leq 0.98$). While these Phase III results are very promising, Clark cautioned that this study does not explicitly highlight the specific clinical applications of this imaging agent. Currently, only a [^{18}F]florbetapir-negative scan is considered clinically useful, as it can help rule out the presence of pathologically significant levels of Aβ in the brain and thus AD pathology. [^{18}F]Florbetapir cannot, however, diagnose AD because cerebral amyloid deposition is not specific to this diagnosis. Due to encouraging results from its Phase III clinical study, Avid Radiopharmaceuticals (now a sub-company under Eli Lilly and Company) filed for FDA approval of [^{18}F]florbetapir in late 2010 (Sullivan, 2011). In a vote of 13-3, the Peripheral and Central Nervous System Drugs Advisory Committee did not recommend approval of [^{18}F]florbetapir in January 2011, citing high inter-reader variability and the lack of a single clinically applicable binary reading method as outstanding issues (Sullivan, 2011). The advisory committee did, however, subsequently vote 16-0 in favor of approval if Avid were to implement reader-training programs (Sullivan, 2011). Such implementation is currently in progress.

The committee's decision was partially based on the results presented in the study by Clark and co-workers (Clark, et al., 2011b). Upon independently analyzing the critical individual reader score data, the FDA found substantial inter-reader variability among independent, extensively trained readers of [^{18}F]florbetapir PET scans for individuals in the autopsy

cohort (Carome and Wolfe, 2011); in particular, sensitivities ranged from 55% to 90%, while specificities were between 80% and 100%. The FDA determined that the readers probably had different thresholds for positive and negative scans on their visual assessment scale; and thus, education initiatives are needed to introduce a consistent binary reading method (Clark, et al., 2011a). In March 2011 the FDA echoed the advisory committee's recommendation in their official response on [18F]florbetapir, requesting that Avid Radiopharmaceuticals work to implement a reader-training program that will lead to better inter-reader reliability. When this issue has been adequately addressed, it is expected that FDA approval will be gained for [18F]florbetapir.

2.4 Imaging tau neurofibrillary tangle burden in Alzheimer's disease
2.4.1 Introduction to tauopathies

Besides amyloid-β, tau is the other hallmark protein that plays a primary role in the pathogenesis of Alzheimer's disease. Tau microtubule-associated protein is essential for maintaining proper neuronal function, but in some individuals this protein can accumulate intraneuronally due to abnormal changes in the regulation of the protein. This process is believed to be the cause of a wide spectrum of different types of dementias known collectively as neurodegenerative tauopathies. In addition to Alzheimer's disease, other common tauopathies in humans include Frontotemporal dementia (FTD), Pick's disease, progressive Supranuclear Palsy (PSP), and Parkinson's disease (Ludolph, et al., 2009), and, unfortunately, many of these diseases are currently not curable.

As addressed above, there is currently no effective way to definitively diagnose AD (or other tauopathy) patients before the disease has done irreversible damage. As is the case with amyloid-β plaques, risky brain biopsies can be used to determine the presence of tau, but *post-mortem* examination of the brain is needed to definitively diagnose these types of disease. While many clinical diagnostic techniques can be used, they require patients to be in moderate to late stages of the disease, a time when treatment is much less effective. New diagnostic techniques, however, are being explored to enable earlier and more definitive diagnosis of AD with PET imaging. While numerous probes have targeted amyloid-β plaques, the most promising possibility is to develop a tau-specific PET biomarker that would improve diagnostic confidence, enable detection of early stages of AD, and allow doctors to monitor the progress of future treatments.

Microtubules are the cytoskeletal components that allow nutrients to be transported far distances along the length of axons. Axoplasmic transport in neurons is an essential process, necessary to maintain proper neuron function. Microtubules however are somewhat unstable and must be stabilized by tau proteins in order to function properly. In normally functioning human brains, tau binds to microtubules to promote stability and polymerization in order to enable axoplasmic flow and preserve overall neuronal functioning. Six tau isoforms exist in the adult human brain, each with an alternative exon splicing sequence. Three of these isoforms, known as 3R-tau are made up of three carboxy-terminal tandem repeat sequences and the other three isoforms, known as 4R-tau consist of four carboxy-terminal tandem repeat sequences. In adult humans the ratio of 3R-tau to 4R-tau is approximately 1:1 (V. M. Y. Lee, et al., 2001). The purpose of these different isoforms is not completely understood. It is known, however, that only the shortest form of 3R-tau is expressed in the fetus, while all six isoforms are expressed in adult brains. One study suggests that the 4R-tau isoform is more effective in promoting microtubule binding than

the 3R-tau isoform. The exact mechanism by which tau is regulated in the brain is also largely unknown; however, recent studies suggest that phosphorylation levels of tau play an important role in tau regulation. Increased phosphorylation of tau likely decreases the ability of the protein to bind to microtubules. For this reason, it is believed that protein kinases and phosphatases play a role in tau regulation. The malfunction of this phosphorylation regulation mechanism is thought to be a major cause of tauopathies. In normally functioning brains, tau proteins contain approximately 2-3 moles of phosphate per mole of tau protein (Iqbal, et al., 2005).

In the case of AD, tau proteins are hyperphosphorylated, which causes a decrease in the ability of the tau to bind to microtubules, leading to microtubule dysfunction and neuronal death. Hyperphosphorylated tau is observed in the plaques of AD patients upon *post-mortem* examination. The mechanism by which this hyperphosphorylated tau is converted into a plaque is currently unknown. One theory for this process is that hyperphosphorylation of the tau causes it to lose binding affinity with microtubules, causing the aggregation of tau into insoluble intraneuronal brain deposits. In all neurodegenerative tauopathies, deposits and tangles of tau proteins are observed in the brain. In AD, tau accumulates in the brain in different structures known as neurofibrillary tangles (NFTs). These NFTs are composed of different structures of tau consisting of paired helical filaments (PHFs) and straight filaments. Tau aggregates are very insoluble in neurons and ultimately cause neuronal death by interfering with the essential axoplasmic flow of nutrients to different cell structures. As so little is known about the cause of Alzheimer's disease and other tauopathies, it is important to develop a better method for studying tau.

2.4.2 PET imaging of tau neurofibrillary tangle burden

Non-invasive functional molecular imaging techniques such as PET imaging have the potential to become the future diagnostic standard for Alzheimer's disease and related tauopathies as they would allow for earlier and more definitive diagnosis of such diseases, and provide an effective method for monitoring possible treatments. One such approach being aggressively explored is the development of tau specific radiopharmaceuticals that would allow for the non-invasive quantification of tau NFTs in the brain. Developing appropriate biomarkers for detecting tau has proven challenging as they must cross the blood brain barrier (BBB), bind selectively to tau, demonstrate safe biodistribution, and exhibit low non-specific binding. Nevertheless, several tau-targeting radiopharmaceuticals, radiolabeled with fluorine-18 or carbon-11, are in various stages of clinical and pre-clinical development. Experimental radiopharmaceuticals including BF-158, FDDNP and T808 are possible candidates for PET imaging of tau, and are outlined below for proof-of-concept purposes.

2.4.2.1 [18F]FDDNP

2-(1-[6-[(2-[18F]fluoroethyl)(methyl)amino]-2-naphthyl]ethylidene)malononitrile ([18F]FDDNP) is a recently developed radiopharmaceutical designed to elucidate brain plaques and NFTs (Small, et al., 2006). Unlike [11C]PiB, [18F]FDDNP can bind to both amyloid-ß plaques as well as tau NFTs, and it has been used in this capacity to quantify NFT and plaque build-up in AD (Small, et al., 2006). Currently [18F]FDDNP is the only biomarker of its kind being studied in human clinical trials, and such trials demonstrated the ability of [18F]FDDNP PET to distinguish healthy control patients from patients with mild cognitive

impairment, and from patients with AD. Initial studies have shown that patients with AD have significantly more [18F]FDDNP binding in the temporal, parietal, and frontal regions of the brain than the corresponding healthy controls. The non-specificity of [18F]FDDNP, however, appears to have limited its application to date, as the study of this probe has not progressed past these initial clinical studies.

2.4.2.2 Quinoline and benzamidizole PET biomarkers

Investigations into the possibility of using radiolabeled quinoline and benzamidizole derivatives for PET imaging of tau NFTs have been reported recently by Okamura and colleagues (N. Okamura, et al., 2005). Initial experiments, with [11C]BF-126, [11C]BF-158, and [11C]BF-170, demonstrated that these compounds have a high affinity for tau NFTs. Furthermore, these compounds appear to bind specifically to tau, without extensive non-specific binding to amyloid plaques. Through the use of *in vitro* staining of AD brain slices, [11C]BF-158 was shown to be the most promising compound for PET imaging of tau NFTs. These radiopharmaceuticals only interact with tau formations in the brains of AD patients. This could prove beneficial for distinguishing early AD from other types of tauopathies. For example, these radiopharmaceuticals do not bind strongly to the tau structures present in the brain slices of patients with Pick's disease and PSP. Although these radiopharmaceuticals have not yet been translated into human clinical trials, the promising pre-clinical data suggest they possess the appropriate properties to make them realistic radiopharmaceuticals for future testing.

2.4.2.3 [18F]T794, [18F]T807 and [18F]T808

Recently, Kolb and colleagues reported development of PET radiopharmaceuticals with high binding affinity and selectivity for tau tangles (Szardenings, et al., 2011), and three lead compounds were identified: [18F]T794, [18F]T807 and [18F]T808. Initial autoradiographical and rodent microPET studies suggest these compounds have the desired binding affinity for tau and good selectivity for tau over amyloid, to fill the void in clinical tau PET imaging. Translation into the clinic is underway, although human imaging studies with these compounds have also yet to be reported.

2.5 Imaging the cholinergic system

The abnormal aggregation of amyloid and tau proteins in AD pathophysiology is accompanied by concomitant decline of neurotransmitter systems, primarily the cholinergic system (Bierer, et al., 1995; Bohnen, et al., 2005; Contestabile, 2011; Francis, et al., 1999; Terry and Buccafusco, 2003). Thus, from a diagnostic perspective, there is interest in being able to image the cholinergic system with PET. To date, efforts have focused upon developing radiolabeled analogs of acetylcholine that are substrates for acetylcholinesterase. Acetylcholinesterase (AChE) is the enzyme responsible for the degradation of acetylcholine, leading to the termination of cholinergic neurotransmission. AChE deficits in *post-mortem* AD brain samples have been observed, suggesting that cholinergic decline is part of the complex neurodegenerative cascade that occurs in AD. Therefore, radiopharmaceuticals suitable for quantifying AChE *in vivo* have potential for tracking the progression of the cholinergic aspect of this cascade in AD patients. The synthetic acetylcholinesterase substrate, 1-[11C]methylpiperidin-4-yl propionate ([11C]PMP) (Shao, et al., 2003; Snyder, et al., 1998), is currently in routine clinical use as a radiopharmaceutical for the study of AChE function in AD patients, and results from such studies have been encouraging (K. A. Frey,

et al., 1997; Iyo, et al., 1997; Koeppe, et al., 1997; Kuhl, et al., 1996). For example, statistically significant decreases in the cortical hydrolysis rate of [11C]PMP in AD brains, versus age-matched controls, have been detected, and correlations identified (Bohnen, et al., 2005; Iyo, et al., 1997; Kilbourn, et al., 1996; Kuhl, et al., 1996). Similar results have also been obtained using [11C]-*N*-methyl-4-piperidyl-acetate ([11C]AMP) (Namba, et al., 1994).

2.6 Measurement of neuroinflammation

Microglial activation is the body's natural response to brain injury and associated neuroinflammation. In addition, microglial activation is also thought to play a significant role in the immune response to AD-related neuronal degeneration and, in AD patients, activated microglia can be found at sites associated with the deposition of aggregated Aβ (Kadir and Nordberg, 2010). There is consequently significant interest in developing radiopharmaceuticals that allow exploration of microglial activation using PET imaging, and the most common are ligands that target the peripheral benzodiazepine receptor including [11C]PK11195 and [11C]PBR28. Cagnin and co-workers reported increased levels of [11C]PK11195 in the entorhinal, temporoparietal, and cingulate cortices in patients with mild AD (when compared to normal controls) (A. Cagnin, et al., 2001). In related work, Edison and colleagues imaged AD patients with both [11C]PK11195 and [11C]PiB. They found a negative correlation between cortical microglial activation and cognition in AD patients, but there was no observable correlation between [11C]PK11195 uptake and [11C]PiB binding (Edison, et al., 2008).

3. Parkinsonian dementias

3.1 Introduction

Parkinson's disease (PD) is a progressive degenerative neurological disease, characterized by asymmetric onset of resting tremors, rigidity, and bradykinesia in the limbs, leading ultimately to unstable posture. The disease is less common in adults under 60, but not unheard of, and it does become more common with increasing age. Progression of symptoms in PD typically occurs over 10–30 years, but progression can be accelerated in certain individuals, especially those with the so-called Parkinson's-plus syndrome.

The hallmark pathology of Parkinson's disease is loss of dopaminergic neurons in the substantia nigra pars compacta (SNc), leading to striatal dopamine deficiency, and classical symptoms of PD are thought to develop when 80% of striatal dopamine and 50% of the SNc neurons are lost. In addition to dopamine loss, concomitant formation of Lewy bodies also occurs in PD. Lewy bodies are composed primarily of synuclein and appearance of such intraneuronal Lewy body inclusions occurs initially in the lower brainstem and medulla oblongata, followed by midbrain and nigral involvement and, eventually, limbic and association cortical areas. Despite this, Pavese and Brooks indicate that even with the prevalence of Lewy bodies, decline of the dopaminergic system is still the primary factor in PD. Other related Parkinsonian syndromes are known however, and dementia occurs in most of them. For example, Dementia with Lewy bodies (DLB) is a common neurodegenerative dementia that is also associated with the development of α-synuclein positive Lewy body neuronal inclusions in the cortex, substantia nigra and brainstem. Patients with DLB, suffer from progressive cognitive decline including memory loss, visual hallucinations, cognitive circadian fluctuations and sleep disorders. Reflecting the seriousness of these conditions, enormous research has been undertaken to develop

numerous radiopharmaceuticals (Figure 3) that can be used to differentiate these conditions and monitor their progression. Progress in this area to date has also been recently reviewed (Pavese and Brooks, 2009; Sioka, et al., 2010).
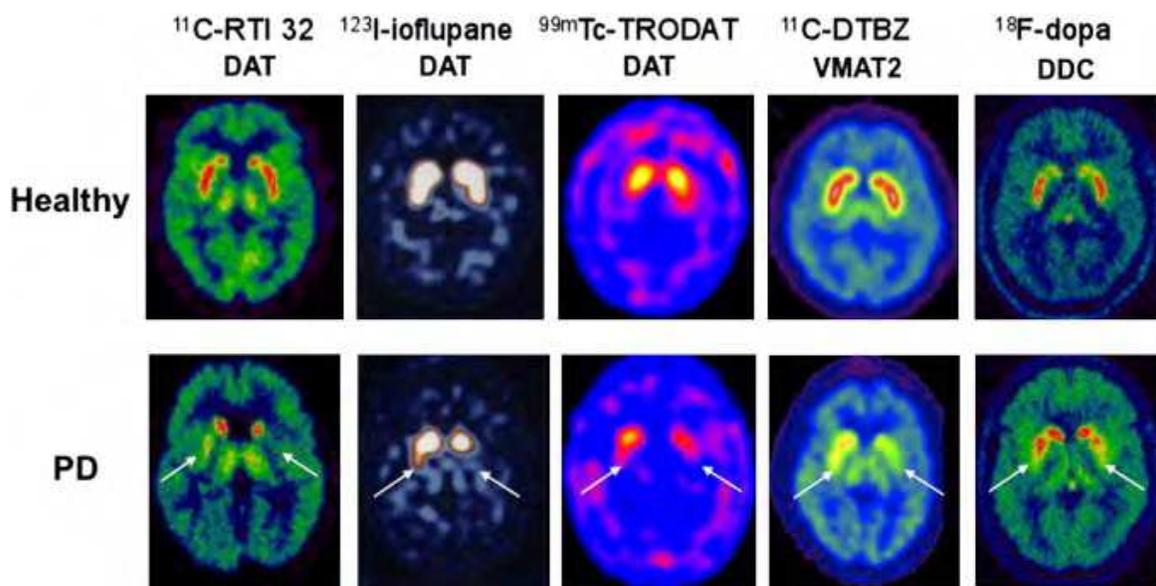

Fig. 3. Imaging dopamine terminal function in healthy controls and early Parkinson's disease. (Reprinted with permission from Pavese N and Brooks DJ, Imaging neurodegeneration in Parkinson's disease. Biochim. Biophys. Acta. 2009;1792:722-729)

3.2 Measurement of striatal aromatic amino acid decarboxylase activity

[^{18}F]DOPA is a radiopharmaceutical used for neuroimaging and for evaluation and quantification of presynaptic dopaminergic integrity. For example, analyzing the uptake of [^{18}F]DOPA in the striatal nuclei provides valuable information on both the density of the axonal terminal plexus and the activity of striatal aromatic amino acid decarboxylase (AADC), an enzyme that converts [^{18}F]DOPA to [^{18}F]dopamine (Pavese and Brooks, 2009). Therefore [^{18}F]DOPA uptake in the striatum of patients with PD is dependent upon the number of remaining dopaminergic cells, and can be used to track progression of the disease. It is worth noting, however, that early degeneration can be underestimated due to compensatory upregulation of AADC in remaining terminals (Ribeiro, et al., 2002).

Significant research has been undertaken to investigate the uptake of [^{18}F]DOPA in the putamen region of the brain, and noticeable [^{18}F]DOPA reductions have been shown to correlate with the clinical severity of rigidity and bradykinesia in PD patients (Brooks, et al., 1990; Broussolle, et al., 1999; Vingerhoets, et al., 1997). However, there is no correlation with the degree of tremors, and Pavese and Brooks highlight that this lack of correlation is suggestive of non-nigrostriatal and/or non-dopaminergic origins of the tremors associated with PD (Pavese and Brooks, 2009). In patients with hemiparkinsonism (i.e. Parkinsonian symptoms on one half of the body only), a corresponding reduction in dorsal posterior putamen uptake of [^{18}F]DOPA on the opposite side of the body has been observed (Morrish, et al., 1995). As the disease progresses to become bilateral, so to does the reduction of [^{18}F]DOPA uptake, and losses are detected in the ventral and anterior putamen and dorsal caudate. In the end stages of the disease, reduced [^{18}F]DOPA uptake in the ventral head of the caudate is also apparent. Such findings also correspond well to *post-mortem* data

(Fearnley and Lees, 1991; Kish, et al., 1988). Beyond these obvious areas of reduced [^{18}F]DOPA uptake, if voxel analysis of the PET scans is performed, then less obvious reductions in [^{18}F]DOPA uptake can also be detected across the entire brain (Kaasinen, et al., 2001; Rakshi, et al., 1999; Whone, et al., 2003).

3.3 Measurement of the Vesicular Monoamine Transporter (VMAT) 2

In neurodegenerative diseases there are typically characteristic losses of particular types of neurons in the human brain. As outlined above, progressive losses of dopaminergic neurons is the hallmark of Parkinson's disease. Reflecting this, a number of strategies have been developed for *in vivo* imaging of such neuronal losses. One such approach involves targeting the vesicular monoamine transporter type 2 (VMAT2) using radioligands such as (+)-α-[^{11}C]dihydrotetrabenazine ([^{11}C]DTBZ: (2R,3R,11bR)-(1,3,4,6,7,11b-hexahydro-9-[^{11}C]methoxy-10-methoxy)-3-(2-methylpropyl)-2-hydroxy-2H-benzo[a]quinolizine) (K. A. Frey, et al., 2001). The VMAT2 is not specific for any monoamine, but is a common protein capable of transporting dopamine, norepinephrine, serotonin and histamine (Eiden and Weihe, 2011). Despite this non-specificity, the utility of VMAT2 imaging in neurodegenerative disease is still possible due to the compartmentalization of neuronal types in the human brain (K. A. Frey, et al., 2001). For example, dopaminergic nerve terminals predominate in the basal ganglia, and so enable specificity for examining losses of such terminals in PD patients (Figure 3). The VMAT2 is found in presynaptic vesicles, and transports monoamines from the cell cytosol into the storage vesicle, from where they can be released into the synapse (Wimalasena, 2011).

Lee and colleagues conducted a comparison between [^{11}C]DTBZ, [^{18}F]DOPA and [^{11}C]methylphenidate (a radiopharmaceutical targeting the dopamine transporter (DAT)) (C. S. Lee, et al., 2000). Reflecting the upregulation of aromatic amino acid decarboxylase, and concomitant down regulation of the DAT, that occurs to increase dopamine turnover and reduce its reuptake in Parkinson's disease patients, this study found that [^{18}F]DOPA Ki was reduced less than the [^{11}C]DTBZ binding potential in the PD striatum, and [^{11}C]DTBZ binding was reduced when compared to [^{11}C]methylphenidate binding. The authors suggest that [^{11}C]DTBZ PET is the most reliable method for quantifying dopaminergic terminal density although, per Pavese and Brooks (Pavese and Brooks, 2009), this needs to be validated and the effect of dopaminergic drugs upon [^{11}C]DTBZ uptake determined.

Reflecting the drive to convert short lived carbon-11 labeled radiopharmaceuticals ($t_{1/2}$ = 20 min) into longer lived fluorine-18 labeled analogs ($t_{1/2}$ = 110 min) to facilitate distribution to satellite PET centers that do not own a cyclotron, [^{18}F]FP-TBZ ([^{18}F]AV-133) has also been developed to image the VMAT2, and is licensed to Avid Radiopharmaceuticals (H. F. Kung, et al., 2008). In studies by Frey and colleagues, AV-133 PET of normal and PD patients were compared (K. A. Frey, et al., 2008). Findings were similar to [^{11}C]DTBZ, and AV-133 PET provided excellent images of the VMAT2. All PD patients had severe reduction of AV-133 accumulation in the striatum, most severe in the PP contralateral to worst PD symptoms. Similar findings were confirmed in further studies by Okamura and co-workers in 2010 (N. Okamura, et al., 2010), and very clear images showing the differences in AV-133 PET between PD patients and healthy controls were obtained (Figure 4).

3.4 Measurement of dopamine transporter binding

The presynaptic dopamine transporter (DAT) is found in dendrites and axons of dopaminergic neurons and is responsible for uptake of dopamine. Therefore, measurement
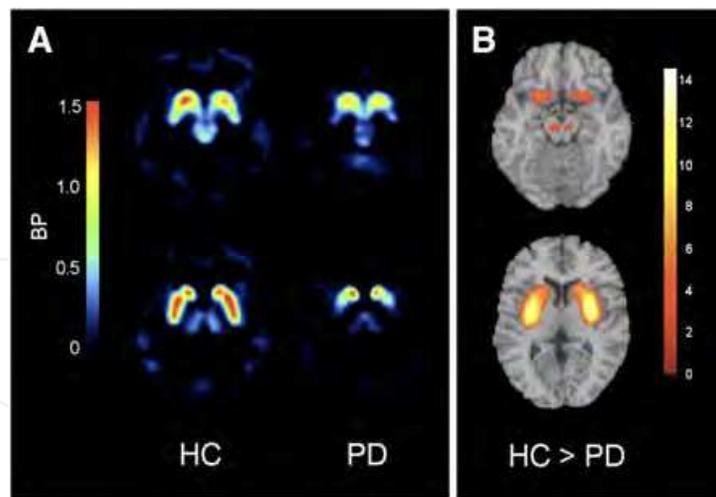
Fig. 4. (A) Representative images of 18F-AV-133 PET BP in HC and PD patient. (B) Areas of reduction in BP of PD patients, compared with HCs, in SPM analysis. Color bars represent t values. P < 0.05, corrected for multiple comparisons. *(Reprinted with permission from Okamura N, Villemagne VL, Drago J, et al. In vivo measurement of vesicular monoamine transporter type 2 density in Parkinson disease with ¹⁸F-AV-133. J Nucl Med. 2010;51:223-228)*

of the DAT can be used as an indicator of the integrity of nigrostriatal projections. Reflecting this, a number of radiopharmaceuticals have been developed that allow for the analysis of DAT activity by PET and SPECT imaging (see the review by Pavese and Brooks for additional information (Pavese and Brooks, 2009)). These include phenyltropane derivatives such as [123]I-ß-CIT (Brucke, et al., 1997; Seibyl, et al., 1995), ^{123}I-FP-CIT ([^{123}I]ioflupane; DaTSCAN) (Castrejón, et al., 2005; Hauser and Grosset, 2011), and [99mTc]trodat (M. P. Kung, et al., 1997), that lead to distinctive images such as those shown in Figure 3. For example, [^{123}I]ioflupane, a radiolabeled analog of cocaine, is approved for clinical use in Europe and the United States, and marketed as DaTSCAN. Nuclear medicine physicians use [^{123}I]ioflupane to diagnose Parkinson's disease (PD), and to differentiate PD from other related neurological disorders that present with similar clinical symptoms (e.g. dementia with Lewy bodies (Antonini, 2007; Castrejón, et al., 2005)). [^{123}I]Ioflupane has a high binding affinity for presynaptic dopamine transporters (DAT). Thus, a SPECT scan conducted using [^{123}I]ioflupane provides physicians with a quantitative measure and the spatial distribution of DAT in the brain. A marked reduction in DAT in the striatal region of the brain is indicative of PD (Figure 3), allowing physicians to diagnose or differentiate a patient's neurological condition with improved diagnostic confidence when compared to diagnosing from clinical symptoms alone.

A review of the two major clinical trials of [^{123}I]ioflupane was recently published by Hauser and Grosset (Hauser and Grosset, 2011). The first study compared baseline scans in patients with early suspected Parkinsonism to the consensus clinical diagnosis established 3 years later (Marshall, et al., 2009). The study found 78-79% positive agreement (abnormal baseline scan and positive diagnosis of PD at 3 yrs, n = 71) and 97% negative agreement (normal baseline scan and negative for PD at 3 yrs, n = 28). The second study was a trial of [^{123}I]ioflupane in patients with established diagnoses of PD or essential tremor (ET), and obtained similar results (Benamer, et al., 2000). This study found 92-97% positive agreement (abnormal baseline scan and positive diagnosis of PD at 3 yrs, n = 158) and 74-96% negative agreement (normal baseline scan and clinical diagnosis of ET, n = 27). Castrejón and

colleagues have also demonstrated that [123I]ioflupane SPECT can distinguish between PD and other Parkinsonian disorders that do not have associated degeneration of the nigrostriatal pathway, such as ET (Castrejón, et al., 2005). Despite these positive findings, it is important to note that an abnormal [123I]ioflupane SPECT scan does not necessarily indicate a diagnosis of PD. Similarly, a normal scan is not entirely indicative of ET (Hauser and Grosset, 2011). In each case, multiple other conditions must be considered and eliminated. For example, abnormal striatal uptake of [123I]ioflupane would be expected in all degenerative Parkinsonian syndromes associated with a loss of nigrostriatal dopamine neurons including PD, progressive supranuclear palsy (PSP), multisystem atrophy (MSA), and corticobasal degeneration (CBD). [123I]Ioflupane SPECT cannot differentiate these related disorders and so, in such cases, it might be necessary to run other tests (FDG PET, PiB PET etc.) to further distinguish such diseases.

3.5 Measurement of neuroinflammation in PD

As discussed above in the context of AD, microglial activation is the body's natural response to brain injury and associated neuroinflammation. Reflecting this, [11C]PK11195 and [11C]PBR28 have been developed to image microglial activation, and recent studies have explored the use of [11C]PK11195 PET in PD patients. Such studies report significant increases in [11C]PK11195 uptake in striatal and extrastriatal regions of PD patients when compared to healthy control subjects (Gerhard, et al., 2006; Ouchi, et al., 2005; Pavese and Brooks, 2009). These findings, which have been correlated with reduced striatal DAT binding (Ouchi, et al., 2005), suggest that significant microglial activation (and associated neuroinflammation) could contribute to dopaminergic neuron loss in PD. This represents an avenue of research that has yet to be extensively explored.

3.6 Imaging of dementia with Lewy bodies

Dementia with Lewy bodies (DLB) is a common Parkinsonian neurodegenerative dementia that is characterized by the development of α-synuclein positive Lewy body neuronal inclusions in the cortex, substantia nigra and brainstem. Patients with DLB, suffer from progressive cognitive decline including memory loss, visual hallucinations, cognitive circadian fluctuations and sleep disorders. In FDG PET of DLB patients, unique hypometabolism in the medial and lateral occipital lobes is observed, and is the feature that distinguishes DLB from AD (Ishii, 2002). DLB can also be distinguished from AD using [18F]DOPA PET. Dopamine deficiencies, similar to PD, have been observed in DLB patients, but not in AD patients (Hu, et al., 2000).

4. Frontotemporal lobe degeneration

4.1 Introduction

Frontotemporal lobe degeneration (FTLD) is a cause of degenerative dementias that recent research suggests, in individuals younger than 65, is as common as AD. Frontotemporal dementia (FTD) is the most common example of such diseases, for which clinical and pathological criteria were proposed in 1994 by Brun and colleagues (Brun, et al., 1994). The disease is characterized by behavioral and personality changes that result from the frontotemporal involvement and include apathy, disinhibition, and often sever impairment of language production. In related conditions, such as semantic dementia and progressive non-fluent aphasia, language impairment can be the major symptom, and dementia the

lesser symptom. In contrast to other dementias however, there is no (or less prominent) memory impairment associated with FTLD. Therefore, clinical differentiation from other diseases such as AD is usually relatively straightforward. The main difficulty associated with managing FTLD is that it is not typically diagnosed in its early stages because mild symptoms often go unnoticed, or are difficult to verify. To address this issue, FDG PET has been investigated as a possibility for diagnosing and staging the FTLD-related conditions by identifying areas of reduced glucose metabolism that are characteristic of these conditions.

4.2 FDG PET for imaging frontotemporal dementia

Reduced glucose metabolism in the frontal (mostly the frontal cortex) and anterior temporal regions is the characteristic hallmark observed in FDG PET scans of FTD patients. Such impairment is not always symmetric, and thought to be related to the aphasia and semantic memory deficits common in such patients. This (mostly) frontal impairment allows distinction of FTD from AD. For example, Foster and co-workers were recently able to distinguish FTD from AD with 86% specificity and 97.6% sensitivity, beyond clinical features alone (Foster, et al., 2007). Frontal metabolic decline, however, is not limited to FTD and can be apparent in certain cases of AD. In such cases where there is FTD / AD overlap in the FDG PET scans, it is recommended to conduct additional scans exploring microglial activation or amyloid deposits (see Section 2). For example, microglial activation characteristic of FTD has been investigated (A. Cagnin, et al., 2004). Alternatively, an amyloid positive scan would strongly suggest AD, whilst an amyloid negative scan would indicate FTD (Figure 5) (Kadir and Nordberg, 2010).
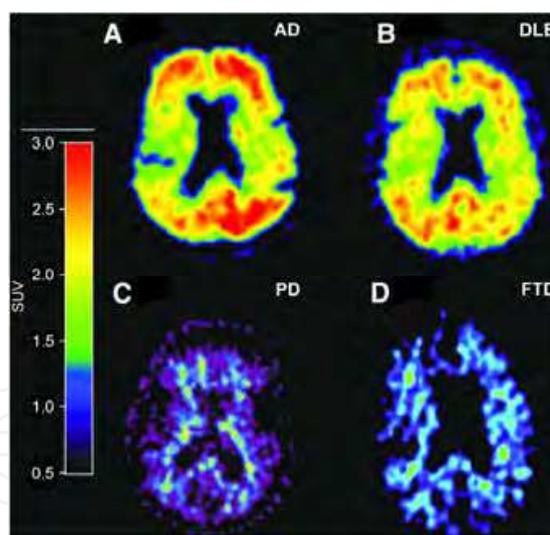

Fig. 5. High PIB retention was observed in patient with AD (A) and patient with DLB (B). In contrast, low PIB retention was observed in patient with PD (not demented) (C) and in patient with FTD (D). *(Parts A and B reprinted with permission from Ahmadul K and Nordberg A, Target-specific PET probes for neurodegenerative disorders related to dementia. J Nucl Med. 2010;51:1418-1430; Part C reprinted with permission from A. Johansson, et al. [11C]-PIB imaging in patients with Parkinson's disease: preliminary results. Parkinsonism Relat. Disord. 2008;14:345-347; Part D courtesy of Professor Henry Engler, Uppsala PET Center, Academical Hospital, Uppsala, Sweden).*

Other diseases (e.g. progressive supranuclear palsy, spino-cerebellar atrophy) or lifestyle choices (e.g. cocaine abuse) can also lead to frontal metabolic impairment. Consequently, other

areas of reduced cerebral glucose metabolism should be considered when making a diagnosis as, despite its name, there are more widespread hemispheric defects in glucose metabolism that occur in FTD. For example, reduced glucose metabolism in the orbital gyrus, anterior cingulate gyrus, frontal cortices, anterior temporal cortices, hippocampus, subcortical structures, parietal region, sensorimotor cortex, and the cerebellar cortex, discussed by Ishii (Ishii, 2002), are consistent with the pathological features and *post-mortem* findings of FTD.

5. Imaging of other dementias

5.1 Corticobasal degeneration

Corticobasal degeneration (CBD) is a progressive dementia in which patients have cognitive decline, significant dementia and unique motor symptoms such as akineto-rigid syndrome (Ishii, 2002). In FDG PET of CBD patients, there is a decrease in absolute glucose metabolism in several regions of the brain, and distinct asymmetry in glucose metabolism patterns that is characteristic of the condition. For example, Hirono and colleagues showed that CBD patients had greater glucose metabolic asymmetries in the lateral frontal, lateral temporal, central and lateral parietooccipital regions than did the corresponding healthy controls (Hirono, et al., 2001). In the same study it was reported that the most significant pathologic changes in CBD appear in the pre- and post-central gyri, and parietal association cortices. Moreover, the associated metabolic asymmetries in the pre- and post-central gyri, as well as the thalamus, were larger in CBD than AD allowing differentiation of these conditions using FDG PET.

5.2 Progressive supranuclear palsy

Progressive supranuclear palsy (PSP) is a condition associated with Parkinsonism and dementia. Pathological changes are most common in the basal ganglia and brain stem, and features of this neurodegenerative condition include behavioral derangement and cognitive decline (Ishii, 2002). In FDG PET of PSP patients, glucose metabolism is reduced in the lateral and medial frontal lobes, caudate nucleus and midbrain, when compared to normal controls (Blin, et al., 1990; Hosaka, et al., 2002).

5.3 Vascular dementia

When dementia results from many small strokes, it is known as vascular dementia. In contrast to other dementias, it is relatively straightforward to diagnose vascular dementia from clinical symptoms, and with MRI or CT. Typically therefore nuclear medicine imaging is not needed for patients with pure vascular dementia (Ishii, 2002). On occasion however, vascular dementia can be associated with AD pathology. In such cases, FDG PET can be employed to distinguish vascular dementia from the reduced glucose metabolism profile associated with AD (see Section 2.2).

6. Conclusion

In conclusion, the sophisticated array of radiopharmaceuticals that have been developed for imaging dementia using PET and SPECT scans is highlighted. Using such imaging techniques alone, or in combination with each other (and/or MRI, CT etc.), allows physicians to differentiate between related, and frequently clinically overlapping, disease entities with a high degree of diagnostic confidence. However, whilst [^{18}F]FDG is readily

available, the more specialized radiopharmaceuticals described herein are still limited to sites typically possessing a cyclotron and advanced radiochemistry laboratories. In order for patients and physicians alike to benefit from these radiopharmaceuticals, global access has to be provided. The new partnerships growing between big pharma, small radiopharmaceutical companies, and larger companies possessing global radiopharmaceutical distribution networks, as well as the appearance of mobile scanner technology, should greatly facilitate access to nuclear medicine imaging in the next decade.

7. Acknowledgement

8. References

Aizenstein, H. J., et al. (2008). Frequent amyloid deposition without significant cognitive impairment among the elderly. *Arch. Neurol.*, Vol. 65, No. 11, (Nov. 2008), pp. 1509-1517, ISSN 00039942.

Anchisi, D., et al. (2005). Heterogeneity of brain glucose metabolism in mild cognitive impairment and clinical progression to Alzheimer disease. *Arch. Neurol.*, Vol. 62, No. 11, (Nov. 2005), pp. 1728-1733, ISSN 00039942.

Antonini, A. (2007). The role of 123I-ioflupane SPECT dopamine transporter imaging in the diagnosis and treatment of patients with dementia with Lewy bodies. *Neuropsychiatr. Dis. Treat.*, Vol. 3, No. 3, (Jun. 2007), pp. 287-292, ISSN 1176-6328.

APA (2000). *Diagnostic and statistical manual of mental disorders (IV-TR), 4th edition* Americam Psychiatric Association, ISBN 978-0890420256, Washington, D.C.

Barthel, H., et al. (2011). Cerebral amyloid-ß PET with florbetaben (18F) in patients with Alzheimer's disease and healthy controls: a multicentre phase 2 diagnostic study. *Lancet Neurol.*, Vol. 10, No. 5, (May 2011), pp. 424-435, ISSN 1474-4422.

Barthel, H., et al. (2010). Individualized quantification of brain ß-amyloid burden: results of a proof of mechanism phase 0 florbetaben PET trial in patients with Alzheimer's disease and healthy controls. *Eur. J. Nucl. Med. Mol. Imaging*, Vol. 49, No. Suppl. 1, (May 2011), pp. 33P, ISSN 1619-7070.

Bartzokis, G., et al. (2007). Human brain myelination and amyloid beta deposition in Alzheimer's disease. *Alzheimer's and Dement.*, Vol. 3, No. 2, (Apr. 2007), pp. 122-125, ISSN 1552-5260.

Bayer (Accessed 2011). *Phase III study of florbetaben (BAY94-9172) PET imaging for detection/exclusion of cerebral ß-amyloid compared to histopathology-NCT01020838.* http://clinicaltrials.gov/ct2/show/NCT01020838 *(accessed May 20, 2011)*

Benamer, H. T. S., et al. (2000). Accurate differentiation of parkinsonism and essential tremor using visual assessment of [123 I]-FP-CIT SPECT imaging: the [123 I]-FP-CIT SPECT study group. *Mov. Disord.*, Vol. 15, No. 3, (May 2000), pp. 503-510, ISSN 0885-3185.

Berent, S., et al. (1999). Neuropsychological function and cerebral glucose utilization in isolated memory impairment and Alzheimer's disease. *J. Psychiatr. Res.*, Vol. 33, No. 1, (Feb. 1999), pp. 7-16, ISSN 0022-3956.

Beyreuther, K. and Masters, C. L. (1991). Amyloid precursor protein (APP) and beta A4 amyloid in the etiology of Alzheimer's disease: precursor-product relationships in

the derangement of neuronal function. *Brain Pathol.*, Vol. 1, No. 4, (Jul. 1991), pp. 241-251, ISSN 1750-3639.

Bierer, L. M., et al. (1995). Neurochemical correlates of dementia severity in Alzheimer's disease: relative importance of the cholinergic deficits. *J. Neurochem.*, Vol. 64, No. 2, (Feb. 1995), pp. 749-760, ISSN 0022-3042.

Blin, J., et al. (1990). Positron emission tomography study in progressive supranuclear palsy. Brain hypometabolic pattern and clinicometabolic correlations. *Arch. Neurol.*, Vol. 47, No. 7, (Jul. 1990), pp. 747-752, ISSN 00039942.

Bohnen, N. I., et al. (2005). Cognitive correlates of alterations in acetylcholinesterase in Alzheimer's disease *Neurosci. Lett.*, Vol. 380, No. 1-2, (May 2005), pp. 127-132, ISSN 0304-3940.

Brooks, D. J., et al. (1990). The relationship between locomotor disability, autonomic dysfunction, and the integrity of the striatal dopaminergic system in patients with multiple system atrophy, pure autonomic failure and Parkinson's disease studied by PET. *Brain*, Vol. 113, No. 5, (Oct. 1990), pp. 1539-1552, ISSN 0006-8950.

Broussolle, E., et al. (1999). The relation of putamen and caudate nucleus 18F-dopa uptake to motor and cognitive performances in Parkinson's disease. *J. Neurol. Sci.*, Vol. 166, No. 2, (Jul. 1999), pp. 141-151, ISSN 0022-510X.

Brucke, T., et al. (1997). Measurement of dopaminergic degeneration in Parkinson's disease with [123I]beta-CIT and SPECT. Correlation with clinical findings and comparison with multiple system atrophy and progressive supranuclear palsy. *J. Neural Transm.*, Vol. 50, No. Suppl., pp. 9-24, ISSN 0300-9564.

Brücke, T., et al. (2000). SPECT and PET imaging of the dopaminergic system in Parkinson's disease. *J. Neurol.*, Vol. 247, No. Suppl. 4, (Sep. 2000), pp. 2-7, ISSN 0340-5354

Brun, A., et al. (1994). Clinical and neuropathological criteria for frontotemporal dementia. *J. Neurol. Neurosurg. Psychiatry*, Vol. 57, No. 4, (Apr. 1994), pp. 416-418, ISSN 0022-3050.

Cagnin, A., et al. (2001). In-vivo measurement of activated microglia in dementia. *Lancet*, Vol. 358, No. 9280, (Aug. 2001), pp. 461-467, ISSN 0140-6736.

Cagnin, A., et al. (2004). In vivo detection of microglial activation in frontotemporal dementia. *Ann. Neurol.*, Vol. 56, No. 6, (Dec. 2004), pp. 894-897, ISSN 0364-5134.

Carome, M. and Wolfe, S. (2011). Florbetapir-PET imaging and postmortem β-amyloid pathology. *J. Am. Med. Assoc.*, Vol. 305, No. 18, (May 2011), pp. 1857, ISSN 0098-7484.

Castrejón, A. S., et al. (2005). 123-I Ioflupane (Datscan) presynaptic nigrostriatal imaging in patients with movement disorders. *Braz. Arch. Biol. Technol.*, Vol. 48, No. Special Issue, (Oct. 2005), pp. 115-125, ISSN 1516-8913.

Choi, S. R., et al. (2009). Preclinical properties of 18F-AV-45: a PET agent for Aβ plaques in the brain. *J. Nucl. Med.*, Vol. 50, No. 11, (Nov. 2009), pp. 1887-1894, ISSN 0161-5505.

Choi, S. R., et al. (2011). Correlation of Amyloid PET Ligand Florbetapir F 18 Binding with Aß Aggregation and Neuritic Plaque Deposition in Postmortem Brain Tissue. *Alz. Dis. Assoc. Dis.*, Vol. 25, No. ASAP On-line, (Mar. 2011), pp. doi: 10.1097/WAD.1090b1013e31821300bc, ISSN 0893-0341.

Clark, C. M., et al. (2011a). Florbetapir-PET imaging and postmortem β-amyloid pathology. *J. Am. Med. Assoc.*, Vol. 305, No. 3, (Jan. 2011), pp. 1857-1858, ISSN 0098-7484.

Clark, C. M., et al. (2011b). Use of Florbetapir-PET for Imaging ß-Amyloid Pathology. *J. Am. Med. Assoc.*, Vol. 305, No. 3, (Jan. 2011), pp. 275-283, ISSN 0098-7484.

Contestabile, A. (2011). The history of the cholinergic hypothesis. *Behav. Brain Res.*, Vol. 221, No. 2, (Aug 2011), pp. ISSN 0166-4328.

de Leon, M. J., et al. (2001). Prediction of cognitive decline in normal elderly subjects with 2-F-18-fluoro-2-deoxy-D-glucose posi- tron-emission tomography (FDG PET). *Proc. Natl. Acad. Sci. USA*, Vol. 98, No. 19, (Sep. 2001), pp. 10966-10971, ISSN 0027-8424.

Drzezga, A., et al. (2008). Imaging of amyloid plaques and cerebral glucose metabolism in semantic dementia and Alzheimer's disease. *Neuroimage*, Vol. 39, No. 2, (Jan. 2008), pp. 619-633, ISSN 1053-8119.

Drzezga, A., et al. (2009). Effect of APOE genotype on amyloid plaque load and gray matter volume in Alzheimer disease. *Neurology*, Vol. 72, No. 17, (Apr. 2009), pp. 1487-1494, ISSN 0028-3878.

Drzezga, A., et al. (2005). Prediction of individual clinical outcome in MCI by means of genetic assessment and (18)F-FDG PET. *J. Nucl. Med.*, Vol. 46, No. 10, (Oct. 2005), pp. 1625-1632, ISSN 0161-5505.

Dubois, B., et al. (2007). Research criteria for the diagnosis of Alzheimer's disease: revising the NINCDS-ADRDA criteria. *Lancet Neurol.*, Vol. 6, No. 8, (Aug. 2007), pp. 734-746, ISSN 1474-4422.

Edison, P., et al. (2008). Microglia, amyloid, and cognition in Alzheimer's disease: an [11C](R)PK11195-PET and [11C]PIB-PET study. *Neurobiol. Dis.*, Vol. 32, No. 3, (Dec. 2008), pp. 412-419, ISSN 0969-9961.

Eiden, L. E. and Weihe, E. (2011). VMAT2: a dynamic regulator of brain monoaminergic neuronal function interacting with drugs of abuse. *Ann. NY Acad. Sci.*, Vol. 1216, No. Addiction Reviews, (Jan 2011), pp. 86-98, ISSN: 0077-8923.

Engler, H., et al. (2006). Two year follow-up of amyloid deposition in patients with Alzheimer's disease. *Brain*, Vol. 129, No. 11, (Nov. 2006), pp. 2856-2866, ISSN 0006-8950.

Engler, H., et al. (2008). In vivo amyloid imaging with PET in frontotemporal dementia. *Eur. J. Nucl. Med. Mol. Imaging*, Vol. 35, No. 1, (Jan. 2008), pp. 100-106, ISSN 1619-7070.

Fagan, A. M., et al. (2007). Cerebrospinal fluid tau/β-amyloid 42 ratio as a predictor of cognitive decline in non-demented older adults. *Neurology*, Vol. 64, No. 3, (Mar. 2007), pp. 343-349, ISSN 0028-3878.

Fearnley, J. M. and Lees, A. J. (1991). Ageing and Parkinson's disease: substantia nigra regional selectivity. *Brain*, Vol. 114, No. 5, (Oct. 1991), pp. 2283-2301, ISSN 0006-8950.

Fodero-Tavoletti, M. T., et al. (2009). Characterization of PiB binding to white matter in Alzheimer disease and other dementias. *J. Nucl. Med.*, Vol. 50, No. 2, (Feb. 2009), pp. 198-204, ISSN 0161-5505.

Fodero-Tavoletti, M. T., et al. (2007). In vitro characterization of Pittsburgh compound-B to Lewy bodies. *J. Neurosci.*, Vol. 27, No. 39, (Sep. 2007), pp. 10365-10371, ISSN 0270-6474.

Forsberg, A., et al. (2010). High PIB retention in Alzheimer's disease is an early event with complex relationship with CSF biomarkers and functional parameters. *Curr. Alz. Res.*, Vol. 7, No. 1, (Feb. 2010), pp. 56-66, ISSN 1567-2050.

Forsberg, A., et al. (2008). PET imaging of amyloid deposition in patients with mild cognitive impairment. *Neurobiol. Aging*, Vol. 29, No. 10, (Oct. 2008), pp. 1456-1465, ISSN 0197-4580.

Foster, N. L., et al. (2007). FDG-PETimproves accuracy in distinguishing frontotemporal dementia and Alzheimer's disease. *Brain*, Vol. 130, No. 10, (Oct. 2007), pp. 2616-2635, ISSN 0006-8950.

Francis, P. T., et al. (1999). The cholinergic hypothesis of Alzheimer's disease: a review of progress. *J. Neurol. Neurosurg. Psychiatry* Vol. 66, No. 2, (Feb. 1999), pp. 137-147, ISSN 0022-3050.

Frey, K. A., et al. (2008). Imaging VMAT2 in Parkinson disease with [F-18]AV-133. *J. Nucl. Med.*, Vol. 49, No. Suppl. 1, (May 2008), pp. 5P, ISSN 0161-5505.

Frey, K. A., et al. (2001). Imaging the Vesicular Monoamine Transporter. *Adv. Neurol.*, Vol. 86, No. pp. 237-247, ISSN 0091-3952.

Frey, K. A., et al. (1997). PET quantification of cortical acetylcholinesterase inhibition in monkey and human. *J. Nucl. Med.*, Vol. 38, No. Suppl. 1, (May 1997), pp. 146P, ISSN 0161-5505.

GEHC (Accessed 2011). *GE Healthcare. Positron Emission Tomography (PET) imaging of brain amyloid compared to post-mortem levels-NCT01165554.* http://clinicaltrials.gov/ct2/show/NCT01165554 *(accessed May 20, 2011)*

Gerhard, A., et al. (2006). In vivo imaging of microglial activation with [11C](R)- PK11195 PET in idiopathic Parkinson's disease. *Neurobiol. Dis.*, Vol. 21, No. 2, (Feb. 2006), pp. 404-412, ISSN 0969-9961.

Greenberg, S. M., et al. (2008). Detection of isolated cerebrovascular β-amyloid with Pittsburgh Compound B. *Ann. Neurol.*, Vol. 64, No. 5, (Nov. 2008), pp. 587-591, ISSN 0364-5134.

Haass, C. and Selkoe, D. J. (2007). Soluble protein oligomers in neurodegeneration: lessons from the Alzheimer' s amyloid β-peptide. *Nat. Rev. Mol. Cell Biol.*, Vol. 82, No. 2, (Feb. 2007), pp. 239-259, ISSN 1471-0072.

Hauser, R. A. and Grosset, D. G. (2011). [123I]FP-CIT (DaTscan) SPECT brain imaging in patients with suspected Parkinsonian syndromes. *J. Neuroimaging*, Vol. No. ASAP On-line, pp. DOI: 10.1111/j.1552-6569.2011.00583.x., ISSN 1051-2284.

Heiss, W. D., et al. (1994). Long- term effects of phosphatidylserine, pyritinol, and cognitive training in Alzheimer's disease. A neuropsychological, EEG, and PET investigation. . *Dementia*, Vol. 5, No. 2, (Mar-Apr. 2004), pp. 88-98, ISSN 1471-3012.

Heiss, W. D., et al. (1992). PET correlates of normal and impaired memory functions. *Cerebrovasc. Brain Metab. Rev.*, Vol. 4, No. 1, (Spring 1992), pp. 1-27, ISSN 1040-8827.

Herholz, K. (2003). PET studies in dementia. *Ann. Nucl. Med.*, Vol. 17, No. 2, (Apr. 2003), pp. 79-89, ISSN 0914-7187.

Herholz, K. (2011). Molecular imaging in Alzheimer's disease. *Eur. Neurol. Rev.*, Vol. 6, No. 1, (Mar. 2011), pp. 16-20, ISSN 1758-3837.

Herholz, K., et al. (2007). Positron emission tomography imaging in dementia. *Br. J. Radiol.*, Vol. 80, No. Special Issue 2, (Dec. 2007), pp. S160-167, ISSN 0007-1285.

Hirono, N., et al. (2001). Neuroral substrates for semantic memory: A positron emission tomography study in Alzheimer's disease. *Dement. Geriatr. Cogn. Disord.*, Vol. 12, No. 1, (Jan-Feb 2001), pp. 15-21, ISSN 1420-8008

Hosaka, K., et al. (2002). Voxel-based comparison of regional cerebral glucose metabolism between PSP and corticobasal degeneration. *J. Neurol. Sci.*, Vol. 199, No. 1, (Jul. 2002), pp. 67-71, ISSN 0022-510X.

Hu, X. S., et al. (2000). 18F-fluorodopa PET study of striatal dopamine uptake in the diagnosis of dementia with lewy bodies. *Neurology*, Vol. 55, No. 10, (Nov. 2000), pp. 1575-1577, ISSN 0028-3878.

Iqbal, K., et al. (2005). Tau Pathology in Alzheimer disease and other tauopathies. *Biochim. Biophys. Acta*, Vol. 1739, No. 2-3, (Jan. 2005), pp. 198-210, ISSN 0006-3002.

Ishii, K. (2002). Clinical application of positron emission tomography for diagnosis of dementia. *Ann. Nucl. Med.*, Vol. 16, No. 8, (Dec. 2002), pp. 515-525, ISSN 0914-7187.

Iyo, M., et al. (1997). Measurement of acetylcholinesterase by positron emission tomography in the brains of healthy controls and patients with Alzheimer's disease. *Lancet*, Vol. 349, No. 9068, (Jun. 1997), pp. 1805-1809, ISSN 0140-6736.

Jack, C. R., et al. (2009). Alzheimer's Diseae Neuroimaging Initiative. Serial PIB and MRI in normal, mild cognitive impairment and Alzheimer's disease: implications for sequence of pathological events in Alzheimer's disease. *Brain*, Vol. 132, No. 5, (May 2009), pp. 1355-1365, ISSN 0006-8950.

Jagust, W. (2004). Molecular neuroimaging in Alzheimer's disease. *NeuroRX*, Vol. 1, No. 2, (Apr. 2004), pp. 206-212, ISSN 1545-5343.

Jellinger, K., et al. (1990). Clinicopathological analysis of dementia disorders in the elderly. *J. Neurol. Sci.*, Vol. 95, No. 3, (Mar. 1995), pp. 239-258, ISSN 0022-510X.

Kaasinen, V., et al. (2001). Increased frontal [(18)F]fluorodopa uptake in early Parkinson's disease: sex differences in the prefrontal cortex. *Brain*, Vol. 124, No. 6, (Jun. 2001), pp. 1125-1130, ISSN 0006-8950.

Kadir, A. and Nordberg, A. (2010). Target-specific PET probes for neurodegenerative disorders related to dementia. *J. Nucl. Med.*, Vol. 51, No. 9, (Sep. 2010), pp. 1418-1430, ISSN 0161-5505.

Kilbourn, M. R., et al. (1996). In vivo studies of acetylcholinesterase activity using a labeled substrate, N[11C]methylpiperdin-4-yl propionate ([11C]PMP). *Synapse*, Vol. 22, No. 2, (Feb. 1996), pp. 123-131, ISSN 0887-4476.

Kish, S. J., et al. (1988). Uneven pattern of dopamine loss in the striatum of patients with idiopathic Parkinson's disease. Pathophysiologic and clinical implications. *New Engl. J. Med.*, Vol. 318, No. 14, (Apr. 1998), pp. 876-880, ISSN 0028-4793.

Klunk, W. E., et al. (2004). Imaging brain amyloid in Alzheimer's disease with Pittsburgh compound-B. *Ann. Neurol.*, Vol. 55, No. 3, (Mar. 2004), pp. 306-319, ISSN 0364-5134.

Klunk, W. E. and Mathis, C. A. (2008). The future of amyloid-beta imaging: a tale of radionuclides and tracer proliferation. *Curr. Opin. Neurol.*, Vol. 21, No. 6, (Dec. 2008), pp. 683-687, ISSN 1350-7540.

Klunk, W. E., et al. (2001). Uncharged thioflavin-T derivatives bind to amyloid-beta protein with high affinity and readily enter the brain. *Life Sci.*, Vol. 69, No. 13, (Aug. 2001), pp. 1471-1484, ISSN 0024-3205.

Klunk, W. E., et al. (2003). The binding of 2-(4'-methylaminophenyl)benzothiazole to postmortem brain homogenates is dominated by the amyloid component. *J. Neurosci.*, Vol. 23, No. 6, (Mar. 2003), pp. 2086-2092, ISSN 0270-6474.

Koeppe, R. A., et al. (1997). Kinetic analysis alternatives for assessing AChE activitiy with N-[C-11]methylpiperidinyl propionate (PMP): to constrain or not to constrain? *J. Nucl. Med.*, Vol. 38, No. Suppl. 1, (May 1997), pp. 198P, ISSN 0161-5505.

Koole, M., et al. (2009). Whole-Body Biodistribution and Radiation Dosimetry of 18F-GE067: A Radioligand for In Vivo Brain Amyloid Imaging. *J. Nucl. Med.*, Vol. 50, No. 5, (May 2009), pp. 818-822, ISSN 0161-5505.

Kuhl, D. E., et al. (1996). Mapping acetylcholinesterase in human brain using PET and N-[C-11]methylpiperidinyl propionate. *J. Nucl. Med.*, Vol. 37, No. Suppl. 1, (May 1996), pp. 21P, ISSN 0161-5505.

Kuhl, D. E., et al. (1982). Effects of human aging on patterns of local cerebral glucose utiliza-tion determined by the [18F]fluorodeoxyglucose method. *J. Cerebr. Blood Flow Metab.*, Vol. 2, No. 2, pp. 163–171, ISSN 0271-678X.

Kukull, W. A., et al. (1990). The validity of 3 clinical diagnostic criteria for Alzheimer's disease. *Neurology*, Vol. 40, No. 9, (Sep. 1990), pp. 1364-1369, ISSN 0028-3878.

Kung, H. F., et al. (2008). Radiolabeled dihydrotetrabenazine derivatives and their use as imaging agents, US 2008/0050312 A1, 45 pp. Vol. No. pp.

Kung, H. F., et al. (2001). Novel stilbenes as probes for amyloid plaques. *J. Am. Chem. Soc.*, Vol. 123, No. 50, (Dec. 2001), pp. 12740-12741, ISSN 0002-7863.

Kung, M. P., et al. (1997). [99mTc]TRODAT-1: a novel technetium-99m complex as a dopamine transporter imaging agent. *Eur. J. Nucl. Med.*, Vol. 24, No. 4, (Apr. 1997), pp. 372-380, ISSN 0340-6997.

Lee, C. S., et al. (2000). In vivo positron emission tomographic evidence for compensatory changes in presynaptic dopamine nerve terminals in Parkinson's disease. *Ann. Neurol.*, Vol. 47, No. 4, (Apr. 2000), pp. 493-503, ISSN 0364-5134.

Lee, V. M. Y., et al. (2001). Neurodegenerative Tauopathies. *Ann. Rev. Neurosci.*, Vol. 24, No. pp. 1121-1159, ISSN 0147-006X

Lin, K. J., et al. (2010). Whole-body biodistribution and brain PET imaging with [18F]AV-45, a novel amyloid imaging agent- a pilot study. *Nucl. Med. Biol.*, Vol. 37, No. 4, (May 2010), pp. 497-508, ISSN 0047-0740.

Lister-James, J., et al. (2011). Florbetapir F-18: a histopathologically validated beta-amyloid positron emission tomography imaging agent. *Semin. Nucl. Med.*, Vol. 41, No. 4, (Jul. 2011), pp. 300-304, ISSN 0001-2998.

Lockhart, A., et al. (2007). PIB is a non-specific imaging marker of amyloid-beta (Abeta) peptide-related cerebral amyloidosis. *Brain*, Vol. 130, No. 10, (Oct. 2007), pp. 2607-2615, ISSN 0006-8950.

Ludolph, A. C., et al. (2009). Tauopathies with parkinsonism: clinical spectrum, neuropathologic basis, biological markers, and treatment options. *Eur. J. Neurol.*, Vol. 16, No. 3, (Mar. 2009), pp. 297-309, ISSN 1351-5101.

Marshall, V. L., et al. (2009). Parkinson's disease is overdiagnosed clinically at baseline in diagnostically uncertain cases: a 3-year European multicenter study with repeat [123 I]-FP-CIT SPECT. *Mov. Disord.*, Vol. 24, No. 4, (Mar. 2009), pp. 500-508, ISSN 0885-3185.

Martins, R. N., et al. (1991). The molecular pathology of amyloid deposition in Alzheimer's disease. *Mol. Neurobiol.*, Vol. 5, No. 2-4, (Jun. 1991), pp. 389-398, ISSN 0893-7648.

Mathis, C. A., et al. (2002). A lipophilic thioflavin-T derivative for positron emission tomography (PET) imaging of amyloid in brain. *Bioorg. Med. Chem. Lett.*, Vol. 12, No. 3, (Feb. 2002), pp. 295-298, ISSN 0960-894X.

Mathis, C. A., et al. (2003). Synthesis and Evaluation of 11C-Labeled 6-Substituted 2-Arylbenzothiazoles as Amyloid Imaging Agents. *J. Med. Chem.*, Vol. 46, No. 13, (Jun. 2003), pp. 2740-2754, ISSN 0022-2623.

McKeith, I. G., et al. (1996). Consensus guidelines for the clinical and pathologic diagnosis of dementia with Lewy bodies (DLB): report of the Consortium on DLB International Workshop. *Neurology*, Vol. 47, No. 5, (Nov. 1996), pp. 1113-1124, ISSN 0028-3878.

McKhann, G., et al. (1984). Clinical diagnosis of Alzheimer's disease—report of the NINCDS–ADRDA work group under the auspices of Department of Health and Human Services Task Force on Alzheimer's disease. *Neurology*, Vol. 34, No. 7, (Jul. 1984), pp. 939-944, ISSN 0028-3878.

McNamee, R. L., et al. (2009). Consideration of optimal time window for Pittsburgh Compound B PET summed uptake measurements. *J. Nucl. Med.*, Vol. 50, No. 3, (Mar. 2009), pp. 348-355, ISSN 0161-5505.

Meyer, P. T., et al. (2011). Dual-biomarker imaging of regional cerebral amyloid load and neuronal activity in dementia with PET and 11C-labeled Pittsburgh Compound B. *J. Nucl. Med.*, Vol. 52, No. 3, (Mar. 2011), pp. 393-400, ISSN 0161-5505.

Minoshima, S., et al. (1997). Metabolic reduction in the posterior cingulate cortex in very early Alzheimer's disease. *Ann. Neurol.*, Vol. 42, No. 1, (Jul. 1997), pp. 85-94, ISSN 0364-5134.

Mintun, M. A., et al. (2006). [11C]PIB in a nondemented population. *Neurology*, Vol. 67, No. 3, (Aug. 2006), pp. 446-452, ISSN 0028-3878.

Morris, J. C., et al. (2009). Pittsburgh Compound B imaging and prediction of progression from cognitive normality to symptomatic Alzheimer disease. *Arch. Neurol.*, Vol. 66, No. 12, (Dec. 2009), pp. 1469-1475, ISSN 00039942.

Morrish, P. K., et al. (1995). Clinical and [18F] dopa PET findings in early Parkinson's disease. *J. Neurol. Neurosurg. Psychiatry*, Vol. 59, No. 6, (Dec. 1995), pp. 597-600, ISSN 0022-3050.

Namba, H., et al. (1994). In vivo measurement of acetylcholinesterase activity in the brain with a radioactive acetylcholine analog. *Brain Res.*, Vol. 667, No. 2, (Dec. 1994), pp. 278-282, ISSN 0006-8993.

Nelissen, N., et al. (2009). Phase 1 study of the Pittsburgh compound B derivative 18F-Flutemetamol in healthy volunteers and patients with probably Alzheimer disease. *J. Nucl. Med.*, Vol. 50, No. 8, (Aug. 2009), pp. 1251-1259, ISSN 0161-5505.

Nordberg, A. (2004). PET imaging of amyloid in Alzheimer's disease. *Lancet Neurol.*, Vol. 3, No. 9, (Sep. 2004), pp. 519-527, ISSN 1474-4422.

Nordberg, A. (2008). Amyloid imaging in Alzheimer's disease. *Neuropsychologia*, Vol. 46, No. 6, (May 2008), pp. 1636-1641, ISSN 0028-3932.

O' Keefe, G. J., et al. (2009). Radiation dosimetry of β-amyloid tracers 11C-PiB and 18F-BAY94-9172. *J. Nucl. Med.*, Vol. 50, No. 2, (Feb. 2009), pp. 309-315, ISSN 0161-5505.

Okamura, N., et al. (2005). Quinoline and Benzimidazole Derivatives: Candidate Probes for In Vivo Imaging of Tau Pathology in Alzheimer's Disease. *J. Neurosci.*, Vol. 25, No. 47, (Nov. 2005), pp. 10857-10862, ISSN 0270-6474.

Okamura, N., et al. (2010). In vivo measurement of vesicular monoamine transporter type 2 density in Parkinson disease with 18F-AV-133. *J. Nucl. Med.*, Vol. 51, No. 2, (Feb. 2010), pp. 223-228, ISSN 0161-5505.

Okello, A., et al. (2009). Conversion of amyloid positive and negative MCI to AD over 3 years. *Neurology*, Vol. 3, No. 10, (Sep. 2009), pp. 754-760, ISSN 0028-3878.

Ouchi, Y., et al. (2005). Microglial activation and dopamine terminal loss in early Parkinson's disease. *Ann. Neurol.*, Vol. 57, No. 2, (Feb. 2005), pp. 168-175, ISSN 0364-5134.

Patt, M., et al. (2010). Metabolite analysis of [18F]Florbetaben (BAY 94-9172) in human subjects: a substudy within a proof of mechanism clinical trial. *J. Radioanal. Nucl. Chem.*, Vol. 284, No. 3, (Mar. 2010), pp. 557-562, ISSN 0236-5731.

Pavese, N. and Brooks, D. J. (2009). Imaging neurodegeneration in Parkinson's disease. *Biochim. Biophys. Acta*, Vol. 1792, No. 7, (Jul. 2009), pp. 722-729, ISSN 0006-3002.

Petersen, R. C., et al. (2009). Mild cognitive impairment: ten years later. *Arch. Neurol.*, Vol. 66, No. 12, (Dec. 2009), pp. 1447-1455, ISSN 00039942.

Pike, K. E., et al. (2007). β-amyloid imaging and memory in non-demented individuals: evidence for preclinical Alzheimer's disease. *Brain*, Vol. 130, No. 11, (Nov. 2007), pp. 2837-2844, ISSN 0006-8950.

Price, J. L. and Morris, J. C. (1999). Tangles and plaques in nondemented aging and "preclinical" Alzheimer's disease. *Ann. Neurol.*, Vol. 45, No. 3, (Mar. 1999), pp. 358-368, ISSN 0364-5134.

Rabinovici, G. D., et al. (2007). 11C-PIB PET imaging in Alzheimer disease and frontotemporal lobar degeneration. *Neurology*, Vol. 68, No. 15, (Apr. 2007), pp. 1205-1212, ISSN 0028-3878.

Rafii, M. S. and Aisen, P. S. (2009). Recent developments in Alzheimer's disease therapeutics. *BMC Med.*, Vol. 7, No. (Feb 2009), pp. 7, ISSN 1741-7015.

Rakshi, J. S., et al. (1999). Frontal, midbrain and striatal dopaminergic function in early and advanced Parkinson's disease. A 3D [18F]Dopa-PET study. *Brain*, Vol. 122, No. 9, (Sep. 1999), pp. 1637-1650, ISSN 0006-8950.

Reiman, E. M., et al. (1996). Preclinical evidence of Alzheimer's disease in persons homozygous for the epsilon 4 allele for apolipoprotein E. *New Engl. J. Med.*, Vol. 334, No. 12, (Mar. 1996), pp. 752-758, ISSN 0028-4793.

Reiman, E. M., et al. (2004). Functional brain abnormalities in young adults at genetic risk for late-onset Alzheimer's dementia. *Prod. Natl. Acad. Sci. USA*, Vol. 101, No. 1, (Jan. 2004), pp. 284-289, ISSN 0027-8424.

Ribeiro, M. J., et al. (2002). Dopaminergic function and dopamine transporter binding assessed with positron emission tomography in Parkinson disease. *Arch. Neurol.*, Vol. 59, No. 4, (Apr. 2002), pp. 580-586, ISSN 00039942.

Rowe, C. C., et al. (2008). Imaging of amyloid β in Alzheimer's disease with 18F-BAY94-9172, a novel PET tracer: proof of mechanism. *Lancet Neurol.*, Vol. 7, No. 2, (Feb. 2008), pp. 129-135, ISSN 1474-4422.

Rowe, C. C., et al. (2007). Imaging beta-amyloid burden in aging and dementia. *Neurology*, Vol. 68, No. 20, (May 2007), pp. 1718-1725, ISSN 0028-3878.

Scheinin, N. M., et al. (2007). Biodistribution and radiation dosimetry of the amyloid imaging agent 11C-PIB in humans. *J. Nucl. Med.*, Vol. 48, No. 1, (Jan. 2007), pp. 128-133, ISSN 0161-5505.

Seibyl, J. P., et al. (1995). Decreased single- photon emission computed tomographic [123I]beta-CIT striatal uptake correlates with symptom severity in Parkinson's disease. *Ann. Neurol.*, Vol. 38, No. 4, (Oct. 1995), pp. 589-598, ISSN 0364-5134.

Shao, X., et al. (2003). *N*-methylpiperidinemethyl, *N*-methylpyrrolidyl and *N*-methylpyrrolidinemethyl esters as PET radiotracers for acetylcholinesterase activity *Nucl. Med. Biol.*, Vol. 30, No. 3, (Apr. 2003), pp. 293-302, ISSN 0047-0740.

Sioka, C., et al. (2010). Recent advances in PET imaging for evaluation of Parkinson's disease. *Eur. J. Nucl. Med. Mol. Imaging*, Vol. 37, No. 8, (Aug. 2010), pp. 1594-1603, ISSN 1619-7070.

Small, G. W., et al. (2006). PET of Brain Amyloid and Tau in Mild Cognitive Impairment. *New Engl. J. Med.*, Vol. 355, No. 25, (Dec. 2006), pp. 2652-2663, ISSN 0028-4793.

Small, G. W., et al. (1995). Apolipoprotein E type 4 allele and cerebral glucose metabolism in relatives at risk for familial Alzheimer disease. *J. Am. Med. Assoc.*, Vol. 273, No. 12, (Mar. 1995), pp. 942-947, ISSN 0098-7484.

Smith, G. S., et al. (1992). Topography of cross-sectional and longitudinal glucose metabolic deficits in Alzheimer's disease. Pathophysiologic implications. *Arch. Neurol.*, Vol. 49, No. 11, (Nov. 1992), pp. 1142-1150, ISSN 00039942.

Snyder, S. E., et al. (1998). Synthesis of 1-[11C]methylpiperidin-4-yl propionate ([11C]PMP) for in vivo measurements of acetylcholinesterase activity,. *Nucl. Med. Biol.*, Vol. 25, No. 8, (Nov. 1998), pp. 751-754, ISSN 0047-0740.

Storandt, M., et al. (2009). Cognitive decline and brain volume loss as signatures of cerebral amyloid-β peptide deposition identified with Pittsburgh Compound B. *Arch. Neurol.*, Vol. 66, No. 12, (Dec. 2009), pp. 1476-1481, ISSN 00039942.

Sullivan, M. G. (2011). FDA panel on amyloid imaging agent: not yet. *Family Practice News*, Vol. 41, No. 3, (Feb. 2011), pp. 15, ISSN 0300-7073.

Szardenings, K., et al. (2011). Novel, small molecule [F18]-PET tracers for imaging of tau in human AD brains. *J. Nucl. Med.*, Vol. 52, No. Suppl. 1, (May 2011), pp. 25P, ISSN 0161-5505.

Tamaoka, A., et al. (1994). Biochemical evidence for the long-tail form (A beta 1-42/43) of amyloid beta protein as a seed molecule in cerebral deposits of Alzheimer's diseae. *Biochem. Biophys. Res. Commun.*, Vol. 205, No. 1, (Nov. 1994), pp. 834-842, ISSN 0006-291X.

Terry, A. V. and Buccafusco, J. J. (2003). The Cholinergic Hypothesis of Age and Alzheimer's Disease-Related Cognitive Deficits: Recent Challenges and Their Implications for Novel Drug Development *J. Pharm. Expt. Ther.*, Vol. 306, No. 3, (Sep. 2003), pp. 821-827, ISSN 0022-3565.

Thal, D. R., et al. (2002). Phases of A-beta deposition in the human brain and its relevance for the development of AD. *Neurology*, Vol. 58, No. 12, (Jun. 2002), pp. 1791-1800, ISSN 0028-3878.

Vandenberghe, R., et al. (2010). 18F-Flutemetamol Amyloid Imaging in Alzheimer Disease and Mild Cognitive Impairment A Phase 2 Trial. *Ann. Neurol.*, Vol. 68, No. 3, (Sep. 2010), pp. 319-329, ISSN 0364-5134.

Vingerhoets, F. J. G., et al. (1997). Which clinical sign of Parkinson's disease best reflects the nigrostriatal lesion? *Ann. Neurol.*, Vol. 41, No. 1, (Jan. 1997), pp. 58-64, ISSN 0364-5134.

Vitali, P., et al. (2008). Neuroimaging in Dementia. *Semin. Nucl. Med.*, Vol. 28, No. 4, (Oct. 2008), pp. 467-483, ISSN 0001-2998.

Whone, A. L., et al. (2003). Plasticity of the nigropallidal pathway in Parkinson's disease. *Ann. Neurol.*, Vol. 53, No. 2, (Feb. 2003), pp. 206-213, ISSN 0364-5134.

Wimalasena, K. (2011). Vesicular monoamine transporters: Structure-function, pharmacology, and medicinal chemistry. *Med. Res. Rev.*, Vol. 31, No. 4, (Jul. 2011), pp. 483-519, ISSN 0198-6325.

Wong, D. F., et al. (2010). In Vivo Imaging of Amyloid Deposition in Alzheimer Disease Using the Radioligand 18F-AV-45 (Florbetapir F 18). *J. Nucl. Med.*, Vol. 51, No. 6, (Jun. 2010), pp. 913-920, ISSN 0161-5505.

Zhang, W., et al. (2007). 18F-labeled styrylpyridines as PET agents for amyloid plaque imaging. *Nucl. Med. Biol.*, Vol. 34, No. 1, (Jan. 2007), pp. 89-97, ISSN 0047-0740.

Zhang, W., et al. (2005a). F-18 polyethyleneglycol stilbenes as PET imaging agents targeting Aβ aggregates in the brain. *Nucl. Med. Biol.*, Vol. 32, No. 8, (Nov. 2005), pp. 799-809, ISSN 0047-0740.

Zhang, W., et al. (2005b). F-18 stilbenes as PET imaging agents for detecting beta-amyloid plaques in the brain. *J. Med. Chem.*, Vol. 48, No. 19, (Sep. 2005), pp. 5980-5988, ISSN 0022-2623.

Ziolko, S. K., et al. (2006). Evaluation of voxel-based methods for the statistical analysis of PIB PET amyloid imaging studies in Alzheimer's disease. *Neuroimage*, Vol. 33, No. 1, (Oct. 2006), pp. 94-102, ISSN 1053-8119.
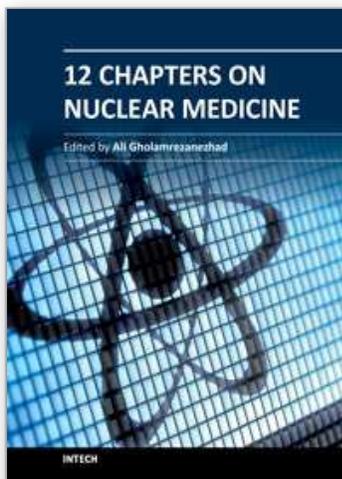
12 Chapters on Nuclear Medicine

Edited by Dr. Ali Gholamrezanezhad

The development of nuclear medicine as a medical specialty has resulted in the large-scale application of its effective imaging methods in everyday practice as a primary method of diagnosis. The introduction of positron-emitting tracers (PET) has represented another fundamental leap forward in the ability of nuclear medicine to exert a profound impact on patient management, while the ability to produce radioisotopes of different elements initiated a variety of tracer studies in biology and medicine, facilitating enhanced interactions of nuclear medicine specialists and specialists in other disciplines. At present, nuclear medicine is an essential part of diagnosis of many diseases, particularly in cardiologic, nephrologic and oncologic applications and it is well-established in its therapeutic approaches, notably in the treatment of thyroid cancers. Data from official sources of different countries confirm that more than 10-15 percent of expenditures on clinical imaging studies are spent on nuclear medicine procedures.

How to reference

In order to correctly reference this scholarly work, feel free to copy and paste the following:

Merissa N. Zeman, Garrett M. Carpenter and Peter J. H. Scott (2011). Diagnosis of Dementia Using Nuclear Medicine Imaging Modalities, 12 Chapters on Nuclear Medicine, Dr. Ali Gholamrezanezhad (Ed.), ISBN: 978-953-307-802-1, InTech, Available from: http://www.intechopen.com/books/12-chapters-on-nuclear-medicine/diagnosis-of-dementia-using-nuclear-medicine-imaging-modalities

INTECH
open science | open minds